Active ankle joints

First prototypes of active ankles released

Work Package	WP2
Del. Rel. No.	D2.5
Del. No.	D7
Title	Active ankle joints
Date	10 Okt. 2019

Contents

Preface vii

Abstract ix

Symbols xi

1 Introduction 1
- 1.1 The THING Project . . . 1
- 1.2 Objective . . . 2
- 1.3 Project Plan . . . 3

2 Literature Research 5
- 2.1 Overview . . . 5
- 2.2 Actuation Mechanisms . . . 6
  - 2.2.1 Direct Rotation . . . 6
  - 2.2.2 Indirect Rotation . . . 8
  - 2.2.3 Indirect Translation . . . 8
- 2.3 Components . . . 12

3 Requirements 13
- 3.1 System Structure . . . 13
- 3.2 List of Requirements . . . 15
- 3.3 Positioning Requirements . . . 15
- 3.4 Other Requirements . . . 18
- 3.5 Requirement Weights . . . 19

4 Conceptual Design 21
- 4.1 Morphological Box . . . 21
- 4.2 Use Value Analysis . . . 22
- 4.3 Motor Sizing . . . 23
  - 4.3.1 Simple Model . . . 23
  - 4.3.2 Detailed Model . . . 26
  - 4.3.3 Candidate Motors . . . 28
- 4.4 Preliminary Design . . . 28
  - 4.4.1 Direct Drive Concepts . . . 28
  - 4.4.2 Tendon Driven Concept . . . 30
  - 4.4.3 Linear Drive Concept . . . 30
  - 4.4.4 Concept Comparison . . . 31
  - 4.4.5 Flat Direct Drive Ankle Version 1 . . . 32
  - 4.4.6 Linear Ankle Version 1 . . . 33
  - 4.4.7 Choice of Concept . . . 33

5 System Design **35**
5.1 Bar Mechanism . . . 35
5.1.1 Simple Model . . . 35
5.1.2 Detailed Model . . . 36
5.1.3 Internal Forces . . . 38
5.1.4 Friction . . . 39
5.2 Design Iterations . . . 40
5.2.1 Linear Ankle Version 2 . . . 40
5.2.2 Linear Ankle Version 3 . . . 41
5.2.3 Linear Ankle Version 4 . . . 42
5.2.4 Linear Ankle Version 5 . . . 44
5.2.5 Final Version . . . 46
5.3 Strength Calculations . . . 46
5.3.1 Bearing Strength . . . 46
5.3.2 Pin Strength . . . 46
5.3.3 Universal Joint Cube Strength . . . 47
5.3.4 Universal Joint Fork Strength . . . 48
5.3.5 Damping Lever Strength . . . 49
5.3.6 Rubber Spring Holder . . . 49
5.3.7 Motor Triangle Strength . . . 50
5.3.8 Shank Adapter Strength . . . 50

6 Alternative Designs **51**
6.1 Linear Ankle . . . 51
6.2 Bowden Ankle . . . 52

7 Production **55**

8 Low Level Control **57**
8.1 Setup . . . 57
8.2 Control over Motion Manager . . . 57
8.2.1 Tuning . . . 57
8.2.2 Homing . . . 57
8.2.3 Back and Forth Movement . . . 58
8.2.4 Compliant Control . . . 59
8.2.5 Dual Control . . . 59
8.3 Control over EtherCAT . . . 60
8.3.1 Connection . . . 60
8.3.2 Control . . . 60

9 Testing **61**
9.1 Range of Motion . . . 61
9.2 Speed . . . 61
9.3 Temperature . . . 64
9.4 Mass . . . 65
9.5 Testing on ANYmal . . . 66

10 Results and Discussion **69**

11 Conclusion and Future Work **71**
11.1 Conclusion . . . 71
11.2 Future Work . . . 71

Bibliography **74**

A Connection Diagram **75**

B Datasheets **77**

Abstract

In this project a new actuated ankle for ANYmal was developed based on an existing passive one. This brings ANYmal one important step closer to being used for inspection of mines and sewers in the THING project, where such new functions will allow it to operate in new and challenging underground environments.
For this, existing robotic ankles were reviewed at the start, after which the requirements and system structure for the new ankle were determined. During a conceptual design process many possible design solutions were explored and narrowed down to the most promising ones. In a further preliminary design step, the remaining candidates were investigated in more detail in the shape of CAD mockups. The final chosen concept uses a linear electric motor with a bar mechanism and was fully realized in CAD. Its motor was chosen through sizing calculations. A second alternative ankle prototype using a bowden cable transmission was also created, after which prototypes of both ankles were manufactured. These were then programmed to perform simple movements simulating their later use. Additionally, interfacing and control via etherCAT with the ankles was enabled. Lastly, they were tested to verify if they fulfilled the requirements defined at the outset.
The results showed that they did fulfill all requirements that could be tested at the time and even exceeded some, most notably in terms of speed, with a repositioning time three times faster than demanded. With some extra work, the ankles will be ready to be used in the THING project and provide a good starting point for future work.

Symbols

Symbols

ϕ	Angle
v	Velocity
a	Acceleration
F	Force
T	Torque
P	Power
σ	Stress
ϵ	Strain
E	Elastic Modulus
S_F	Safety Factor
m	Mass

Indices

x	x axis
y	y axis

Acronyms and Abbreviations

ETH	Eidgenössische Technische Hochschule
RSL	Robotic Systems Lab
IMU	Inertial Measurement Unit
THING	subTerranean Haptic INvestiGator
ROM	Range of Motion
CAD	Computer Aided Design
EOM	Equations of Motion
CFRP	Carbon Fiber Reinforced Polymer
DOF	Degree of Freedom
F/T	Force/Torque
ROS	Robotic Operating System
RMS	Root Mean Square
FBD	Free Body Diagram

Chapter 1

Introduction

1.1 The THING Project

This thesis is part of the THING project, which stands for subTerranean Haptic INvestiGator and will fulfill one of its deliverables. The THING project aims to use robots for inspections of sewers and mines. Specifically the sewage system of the city of Zurich and a mine in Poland (Fig. 1.1). Both of these underground environments are challenging for humans and robots alike. With no natural sunlight and foggy air, visibility is limited. And uneven and wet ground makes walking difficult. Narrow passageways without light mean one has to duck and carry lights and workers have to don protective wear in case of falling debris and to stay clear of smelly polluted water. All in all, these make for very unfriendly working conditions for people, who have to stay in the dark for hours and in some cases need multiple people to keep in radio contact and guide them through the underground maze.

(a) mine (b) sewer

Figure 1.1: environments

This is why one wants to send robots to these places where humans do not want to go. But as for humans, these environments are still tricky for robots, which is why a robot with new capabilities will be developed in this project. ANYthing is based on ANYmal, the quadruped robot from ETH Zurich, with new modifications for underground operation. It will have new articulating feet (Fig. 1.3) instead of only unmoving point contact feet. These will help ANYthing find a stable foothold on bumpy terrain or rocks and will have more grip in wet gravelly areas with a profiled sole. In this dingy workplace, THING will not be able to rely on its visual senses as much, because moisture droplets in the air and darkness will lead to poorer

measurements. Instead, the feet will have new haptic sensing capabilities. Through accelerometers in the sole the ground roughness can be measured by running the sole along it and recording the vibrations. Similarly, ANYthing will be able to inspect machines and measure their vibrations and sense friction coefficients of the ground. Integrated force/torque sensors in the shank will allow it to sense the security of its current stance and push against objects in a controlled manner. The articulating feet could also be used by the THING to stabilize itself against walls or low ceilings. It can also probe cracked walls to check their stability.

Figure 1.2: ANYthing

An envisioned use case for inspection of conveyor belts in the mines is shown in Fig. 1.3. Where ANYthing would make a tour around the belt and take haptic measurements near the rollers and take readings of the motors along the way.

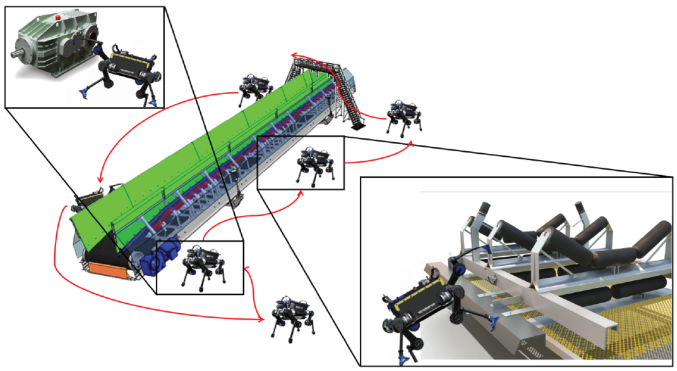

Figure 1.3: Use case

1.2 Objective

New foot designs are essential for the THING project, which is why various different types are being investigated and developed by the involved parties. These include passive feet, feet that mechanically adapt to the ground curvature and actively actuated ankles, the first of which will be developed here. It will be based on a passive foot that has been previously developed at ETH. Fig. 1.4 shows the latest

passive foot at that time. It consists of a CFRP shank, a force/torque sensor and IMU in orange and a foot with rubber sole and integrated IMU. Between foot and shank sits a cylindrical rubber spring (not shown in the Figure) that holds the foot in neutral position, while allowing for passive pitch and roll. Surrounding that is a rubber bellow (not shown) for ingress protection.

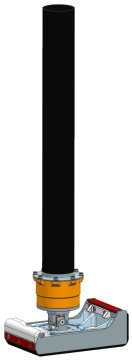

Figure 1.4: Passive foot

The new foot with active ankle serves three main purposes. Firstmost to support the weight of ANYmal, while secondly holding securely on rough terrain without slipping. And lastly it should be able to position the sole at an angle of choice to step on uneven ground and make haptic inspections. The active movement is also required for walking on steep ground, wobbly rocks or when the robot stumbles.
From the task description, the ankle should have the ability to actively control its pitch, while still moving the roll axis passively. The pitch movement is more important when walking and the foot is longer in pitch direction, which is why this direction is more valuable. Having actuated pitch allows the foot to be aligned with any bumpy terrain or rocks, so that the foot can be lowered straight onto it. With a passive ankle extra force must be put onto that foot, which might not always be possible. For instance when reaching up a high ledge. This force might also knock over a rock or other unstable object it wants to step on to. It also allows the foot to move out of the way of obstacles when reaching into small gaps. The ankle is not required to be able to lift up the entire weight of ANYmal on its own, because that would lead to a to large and heavy ankle. Instead it should be repositioned during the flight phase and passively follow ANYmals movements during contact. All the while the ankle has to be able to withstand the environmental conditions, such as water, dirt and sand.

1.3 Project Plan

At the start, the project was planned out week by week for the entire six months (Fig. 1.5). For this it was divided into major stages preceding milestones. The first stages cover the mechanical design, from conceptual to detail design, while the later ones encompass control and testing. In the end the project went according to plan, save for some natural shuffles and changes, and ended on time.

Workpackage	Task #	Task description	START	DURATION
(Add name)	(add task	(Add name of task or MS)		
Concept	1.1	Set up Gantt-Chart	40	1
	1.2	General Literature Research	40	2
	1.3	Components Literature Research	41	2
	1.4	Requirements	42	1
	1.5	Evaluation of mechanical variants	43	1
	1.6	Evaluation of motor variants	43	1
	1.7	Evaluation of electronics	43	1
	1.8	Generation and Evaluation of overall Concepts	44	1
	M1	**Choice of concept**	44	1
Design	2.1	CAD: Create (different) Designs (same concept)	45	1
	2.2	Quick Prototypes, iterate	46	2
	2.3	Choose best design	47	1
	2.4	Choice of motors	48	1
	2.5	Choice of electronics	48	1
	2.6	CAD: Refined final Design	49	3
	2.7	Choice of mechanical components	49	3
	2.8	Mechanical Analysis/Simulation	50	1
	2.9	CAD: Technical Drawings	1	1
	M2	**CAD model, Tech. Drawings, Parts List**	1	1
		Christmas, New year	52	1
Manufacturing	3.1	Order electronics	2	1
	3.2	Order mechanical parts	2	1
	3.3	Machine parts in workshop	2	1
	3.4	Intermediate Presentation, Report	3	1
	3.5	Receive electronics	3	1
	M 3	**Parts ordered and machined**	3	1
	4.1	Set up environment	4	1
	4.2	Assembly electronics and motors	4	1

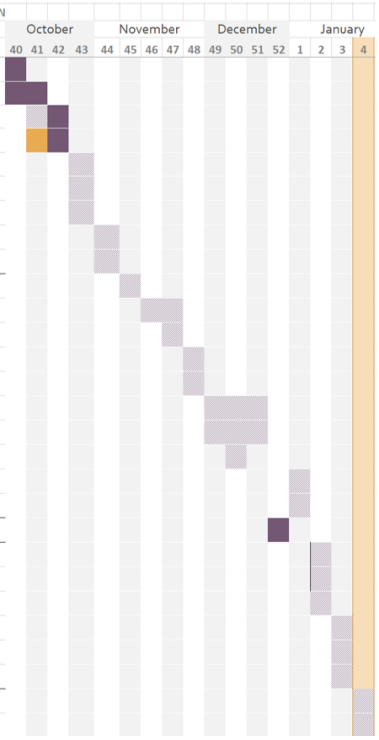

Figure 1.5: Time plan part 1

Workpackage	Task #	Task description	START	DURATION
(Add name)	(add task	(Add name of task or MS)		
Software: Set up	4.3	Test Motors, electronics	4	1
	4.4	Simple position control program	4	2
	4.5	Interface to Anymal	5	1
	M 4	**Simple software & motors ready**	5	1
Assembly	5.1	Receive mechanical parts	5	1
	5.2	Mechanical assembly	6	1
	M 5	**System integrated**	6	1
Software: Position Control	6.1	Test previous program on hardware	6	1
	6.2	Improve and refine software	6	2
	M6	**Position controllable ankle**	7	1
Testing	7.1	Organize Test Setup	7	1
	7.2	Actuation testing	8	1
	7.3	Physical Robustness testing	8	1
	7.4	Waterproofing testing	8	1
	M7	**Results for presentation/report**	8	1
Presentations Report Hand-In	8.1	Prepare Final Presentation	9	1
	8.2	Test Run	9	1
	8.3	Final Presentation	10	1
	8.4	Preliminary Report	41	12
	8.5	Final Report	12	2
	8.6	Prepare Hand-In	13	1
	M8	**Hand-In 3.4.19 (17.4.19 deadline MyStudies)**	14	1

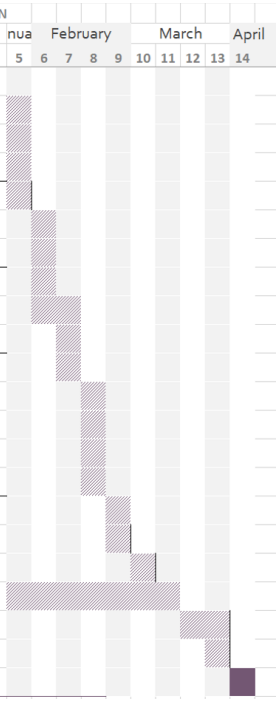

Figure 1.6: Time plan part 2

Chapter 2

Literature Research

2.1 Overview

Robotic ankles mostly occur in two types of robotic systems. In legged robots, but also in robotic prostheses or exoskeletons. The robots are entirely standalone, while the latter augment humans. Depending on the number of legs, the legged robots typically mimic different living beings. Bipedal robots are generally humanoid, quadrupeds similar to cats, dogs etc. Robots with more legs are often arachnoid or insectoid.
Legged robots use either single or multi-point contact feet [1]. Single-point contact feet as can be found on ANYmal (Fig. 2.1) are light, simple to build and agnostic to most angles at which they land. They are also easy to model by approximating them as single points. However, these feet do not provide much surface for gripping on to terrain and have next to no sole profile.

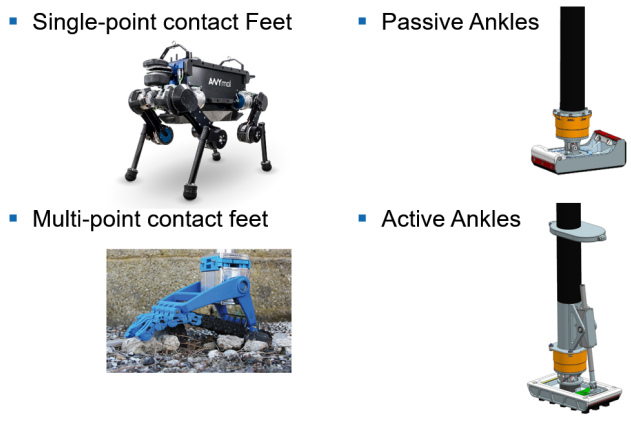

Figure 2.1: (clockwise) ANYmal with single-point contact feet, passive ankle, active ankle, SoftFoot [2]

Multi-point contact feet on the other hand remedy these weaknesses. In trade they are more complex, heavier and harder to model. Feet lacking ankle actuation are passive, such as the PISA SoftFoot (Fig. 2.1). Instead, the ankle may be held in place by springs or the like. Additionally, SoftFoot is adaptive, meaning that it changes its structure and conforms to the shape of the ground. On flat ground the sole stays flat, while it curves when standing on obstacles [2]. Non-adaptive feet simply keep their shape in all situations. Passive feet tend to be lighter because

they need no complex actuation system and are simpler overall. They naturally also require no power consumption.
Active feet use actuators to move their ankle joints and can therefore control their angle to match the ground. This can be achieved with many different approaches, using different actuator and transmission combinations. The next section showcases existing active ankles categorized by these actuation mechanisms.

2.2 Actuation Mechanisms

The mechanisms found in existing active ankles have been categorized by how the rotation of the ankle is achieved (2.2). Either it is rotated directly or indirectly via a transmission, or a transmitted linear movement pushes a lever that moves the joint.

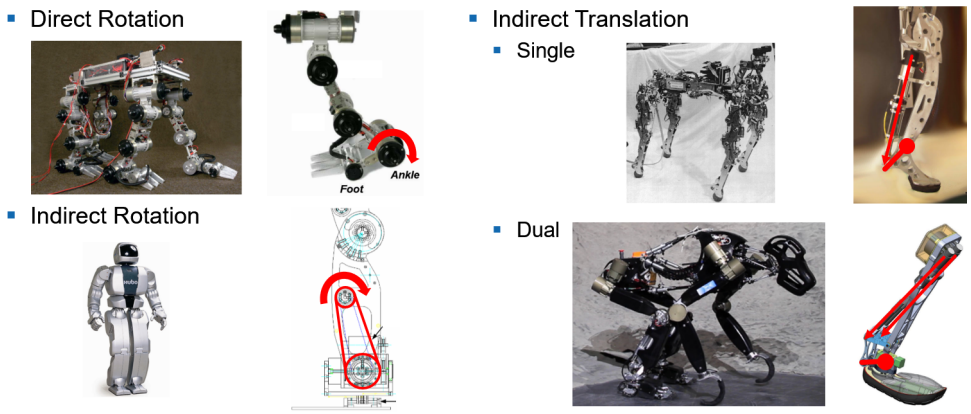

Figure 2.2: Overview of actuation mechanisms [3],[4],[5],[6],[1]

2.2.1 Direct Rotation

The most straightforward method simply embeds the rotary actuator directly into the joint, while a mechanical support structure around it handles all other loads. This can be found in the quadruped ARAMIES (Fig. 2.3), where an electric motor with combined gearhead is embedded into the axis. The ankle has a single pitch DOF. With 28 kg ARAMIES has a similar weight to ANYmal (30 kg) [3].

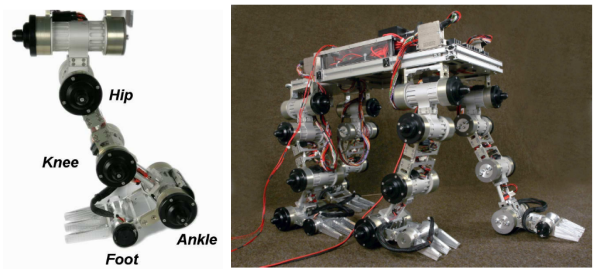

(a) Ankle (b) Robot

Figure 2.3: ARAMIES [3]

In contrast the humanoid cCub has both active pitch and roll axes, where roll is achieved through direct rotation. It uses harmonic drives and brushless, frameless

motors. Additionally a six DOF F/T sensor is in the sole, similar to the ANYmal passive ankle [7].

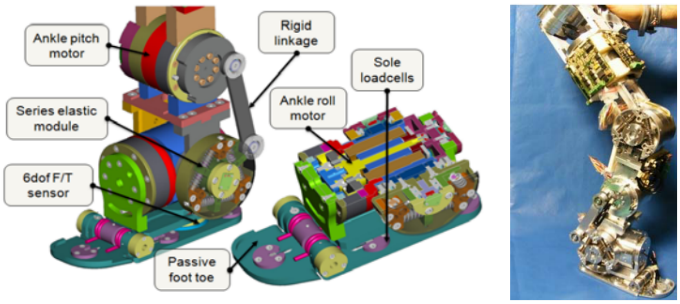

(a) Ankle (b) Leg

Figure 2.4: cCub [7]

SILO2 (Fig. 2.7) also has both axes actuated and roll directly. In this case long DC servomotors are employed [8].

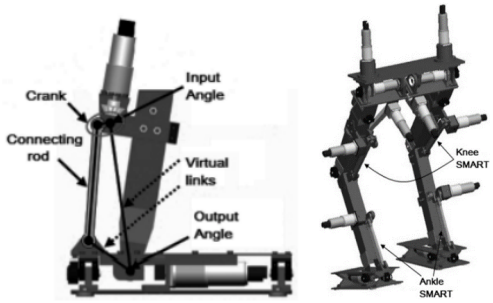

(a) Ankle (b) Robot

Figure 2.5: SILO2 [8]

The mostly planar seven-linked biped robot (Fig. 2.6) has brushed DC motors with planetary gears inside its pitching ankles. They do however protrude substantially [9].

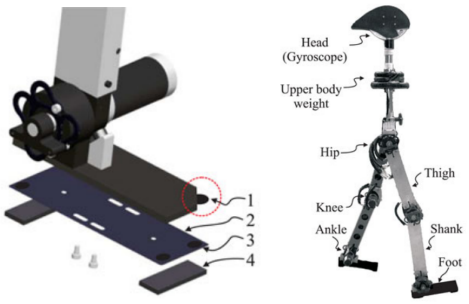

(a) Ankle (b) Robot

Figure 2.6: Seven-linked biped robot [9]

2.2.2 Indirect Rotation

With indirect rotation, the actuator is outside the joint and the rotation transferred via a transmission. This was found in HUBO in Fig. 2.7. Its ankle is actuated in pitch and roll, both of which use brushed DC motors in concert with belt transmissions [4].

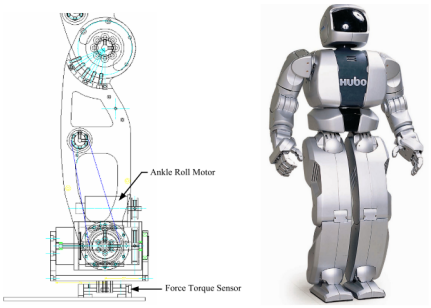

(a) Ankle (b) Robot

Figure 2.7: KHR-3: HUBO [4]

2.2.3 Indirect Translation

Indirect translation mechanisms result in a linear movement near the heel, pushing the foot up and down to make it move. Here they have been sorted by whether they use a single movement at the heel to just actuate one DOF or two for more power and DOFs.

Single movement

The quadruped BISAM has single DOF pitching ankles actuated by DC servos and ball screws attached to the heel. It additionally uses spur gears and features feet shaped similarly to horse hooves [5].

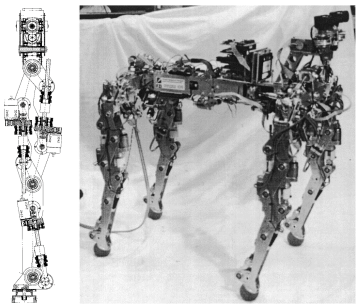

(a) Leg (b) Robot

Figure 2.8: BISAM [5]

The next example is the horse-like HADE leg. It also has one pitch DOF but uses a series elastic actuator including a brushless DC motor. The SEA uses a ball screw in tandem with die compression springs, which allow the ankle to be force controlled and improve its shock tolerance. Another interesting feature of the leg is the use

of a rotary magnetorheological brake in the knee joint. This allows them to control the joint damping and features fast and high-resolution braking [6].

Figure 2.9: HADE [6]

cCub shown previously in Fig. 2.4 uses indirect translation for its second pitch DOF. There the motor is connected via a rigid bar mechanism to the joint. In addition, a series elastic module is mounted at the pitch joint, for extra compliance and damping. Similarly, SILO2 (Fig. 2.7) also achieves its pitch through a four-bar linkage mechanism. In this case the motor drives a crank over bevel gears, which then connects to the heel. This assembly leads to a non-linear transmission ratio between input and output angles.
The bipedal robot in Fig. 2.10 uses a complex spring windup and release system to actuate its single pitch axis. Connected by wires, the motor tensions the spring until it is mechanically locked. Upon release, the foot springs back controlled solely through the spring force. Here a rotary electric motor is used for windup and a solenoid for release [10].

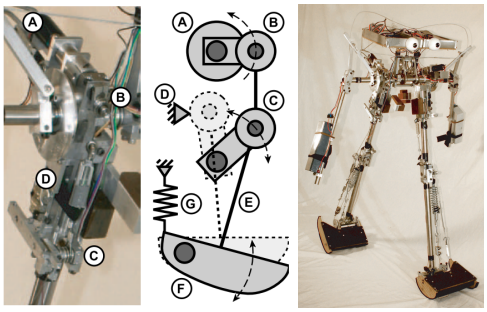

(a) Mechanism (b) Robot

Figure 2.10: Bipedal Robot[10]

The powered ankle foot prosthesis uses a system consisting of a motor, belt transmission, ball screw and spring mounted in series for pitching. In Fig. 2.11, the green belt can be seen connected to the brushed DC motor. The belt drives the ball screw like a lever, to which lastly the helical spring is connected for SEA behavior. On top of that, unidirectional springs are mounted in parallel over a pulley cable mechanism [11].
The BLEEX exoskeleton is one of the few ankles that uses hydraulic actuation. It uses a linear piston at its shin for pitch and has a passive roll axis. They chose linear hydraulics, because rotary ones have internal leakage and friction. The hydraulics also allow them to a achieve high specific power needed in exoskeletons and give high control bandwidth [12].

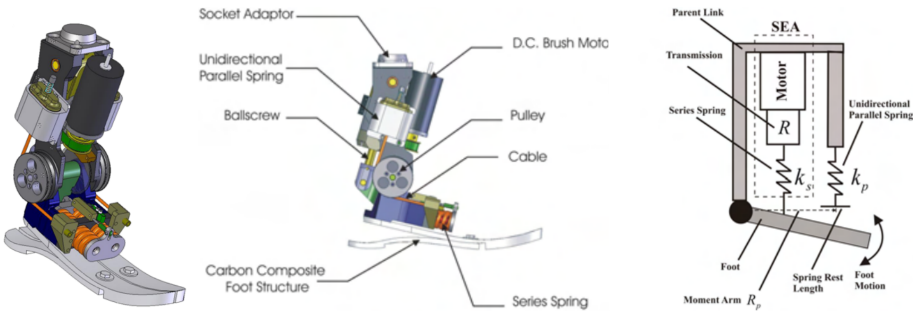

(a) Ankle (b) Mechanism

Figure 2.11: Powered ankle foot prosthesis [11]

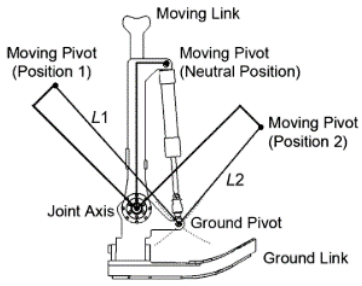

Figure 2.12: BLEEX [12]

Dual Movement

Having two actuators allows the following ankles to have double the pitching force and if arranged in a differential manner, allows simultaneous control of the roll axis. This is the case for the ape-like hominid robot in Fig. 2.13, where two brushless DC motors with lead screws are mounted at the calves. Through a relatively complex multi-link joint mechanism, the ankle has two active DOFs. When both motors move in the same direction, the ankle pitches and otherwise it rolls. This also provides the extra pitching power needed for this 21.5 kg robot [1].

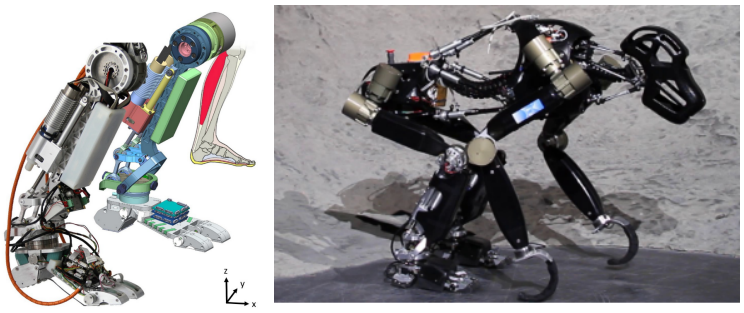

(a) Ankle (b) Robot

Figure 2.13: Hominid robot [1]

The biped jogging robot and ROBIAN use the same differential actuation mechanism (Figs. 2.14, 2.15). The jogging robot additionally uses sliding rods along linear bearings in the transmission, whereas ROBIAN employs a belt drive between

motor and ball screw [1][13].

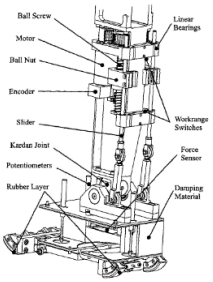

Figure 2.14: Biped jogging robot [1]

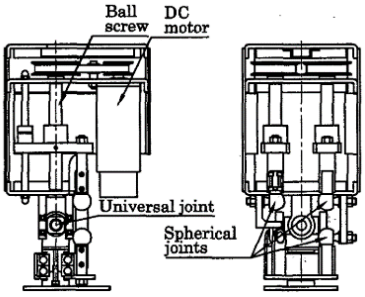

Figure 2.15: ROBIAN [13]

SPARKy 3 (Fig. 2.16) sees this method applied to a prosthesis. It additionally has series elastic actuation in both axes. For pitch helical springs are connected via an L-shaped bar, while inside the roll joint torsion springs with angle limits are integrated [14].

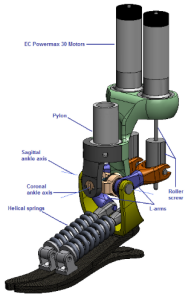

Figure 2.16: SPARKy 3 [14]

On the other hand, the ankle robot for gait rehabilitation (Fig. 2.17) uses bevel gears combined with a four-bar linkage to achieve active pitch and roll. It also allows yaw movement of the subject, with $\pm 15°$ similar to the human ankle's limits [15].
Though not an ankle, the robonaut hand also uses a differential mechanism in its wrist, with linear sliders and ball screws [16].
Lastly, the parallel ankle exoskeleton for rehabilitation uses not two but three motors in parallel arrangement. It can achieve active pitch and roll, though this arrange-

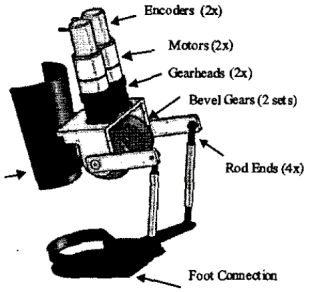

Figure 2.17: modular [15]

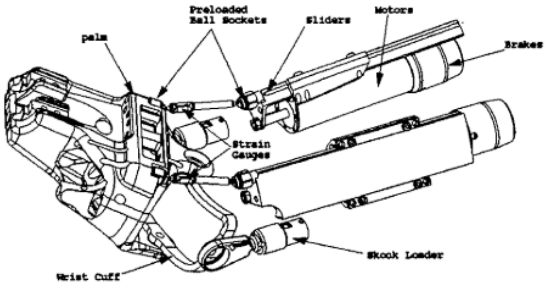

Figure 2.18: The Robonaut Hand [16]

ment leads to complex kinematics and control [17]. With such a setup, vertical translation might also be possible.

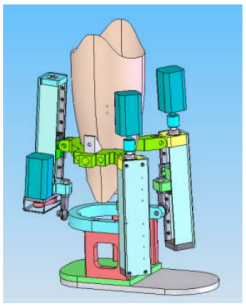

Figure 2.19: Parallel ankle [17]

2.3 Components

In the existing ankles, most of the actuators used were brushed or brushless DC motors. And the transmissions typically ranged from spur and planetary gearheads to ball screws. Nonetheless any other components that would come into question were researched. This included different actuators, such as rotary or linear electromechanical ones, as well as SMA and electrochemical actuators. Furthermore various transmissions including gears were looked, as well as options for actuation mechanisms, spring/damping systems and sensors.

Chapter 3

Requirements

Having gained an overview over existing active ankles in the preceding chapter, it was now possible to proceed to the high-level design phase. This meant breaking down the system structure and determining the requirements for the application and the degree thereof, allowing one to then look for a solution that would meet them as best possible.

3.1 System Structure

The actuated ankle system structure was analysed at from multiple viewpoints. First from an external point of view on the level of the entire robot and the environment in Figure 3.1. Here the ankle is split into its active and passive parts and the relationships between it and the rest of the leg and environment are shown.

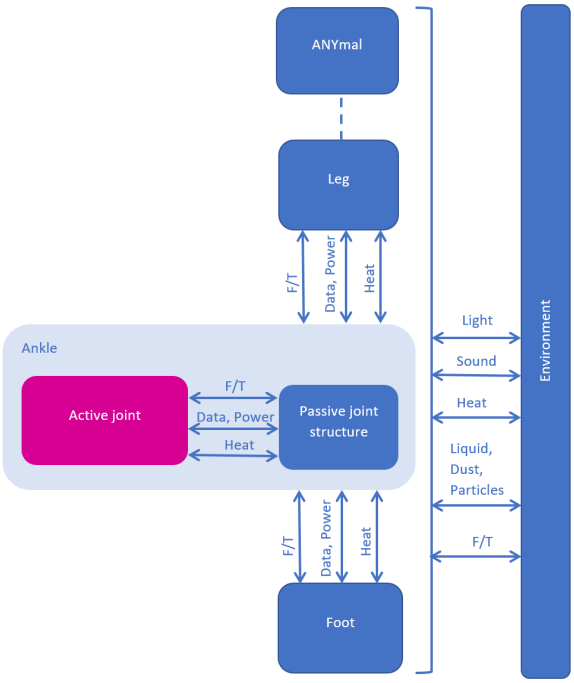

Figure 3.1: External system structure

Then just the active joint itself was analysed in Fig.3.2 with its internal structure

showing all necessary components.

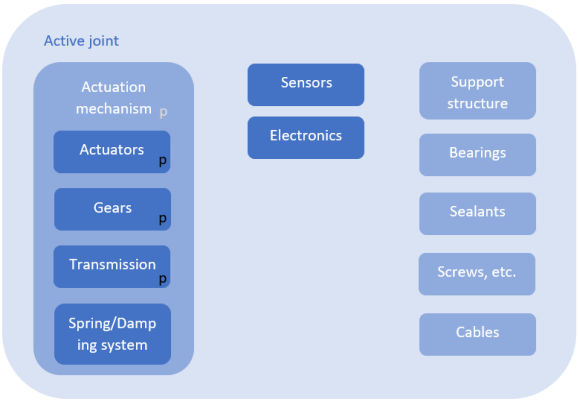

Figure 3.2: Internal system structure, p: only needed for pitch

Lastly, the functions that each of these components must provide were listed in more detail in the functional structure (3.3). This would help to define the requirements and subfunctions later on in the morphological box.

Component	Function

Actuator(s)	• Create rotational (T and w) or linear movement (F and v) to position foot around pitch:
	  ○ Move foot to a different angle
	  ○ Hold foot at the same angle
	  ○ Comply when in ground contact

Gears	• If necessary, amplify or reduce T and w output of the actuator according to gear ratio • If necessary, change axis of rotation
Transmission	• If necessary, transmit the movement created by the actuators to the ankle pitch axis, at any roll position • If necessary, transform the movement created by the actuators to a rotation at the ankle pitch axis, at any roll position • If necessary, amplify or reduce T and w output of the actuator according to gear ratio
Spring/Damping system	• Damp sudden rotations around pitch or roll caused by impact loads • Comply when in ground contact (not strictly necessary for pitch) • For roll axis: ○ Return foot to center angle and hold

Sensors	• Measure the absolute position and velocity of both (if there are losses due to transmission) or one (if one can be inferred by the other) of:
	  ○ actuator
	  ○ ankle pitch
	• Measure the absolute position and velocity of ankle roll
	• Measure F/T if not done by passive structure
	• If necessary, Temperature, for the case that the motor gets hot and influences other sensors

Electronics	• Determine the necessary motor control signal based on sensor signals • Supply the motor with I/V according to control signal • Power all sensors and read out their signals • If necessary, process the signals further

Figure 3.3: Functional structure pt.1

Figure 3.4: Functional structure pt.2

3.2 List of Requirements

The requirements were on one hand based on existing ones set by the THING project, on the other they were determined and set independently in cases arising specifically with this project's ankle. Figure 3.6 lists all of these, categorized into functional, performance and design requirements. Because the actuated ankle is based on the passive one, the requirements pertaining to that existing design are not listed, such as requirements for force sensing capabilities.

3.3 Positioning Requirements

One of the most essential requirements is the speed with which the foot can be repositioned around the pitch axis. It should be able to move through its entire range of motion during the duration of a typical step, that is the time between the foot lifts off and touches down again. On top of that, it should be able to move even faster, to be able to quickly react to unplanned events, such as if ANYmal were to slip or start to fall over.
In order to determine this step time, a set of videos of ANYmal walking was analyzed. Clips from RSL YouTube videos were chosen with a point of view looking as straight on to the side of ANYmal as possible. This resulted in two clips, one showing typical walking speed and the other the fastest occurring speed amongst all seen videos. Both were then analyzed in Kinovea, a program for sports video analysis, allowing video overlays for tracking of angles and other metrics. Figure 3.7 shows timestamped frames from the first walking case of both lift-off and touch-down of one foot, along with the shank angle at those moments. The angle measurements allowed one to later calculate the rough angular speed of the shank, which helped in estimating the needed motor specifications. Correspondingly, Figure 3.8 shows the fast case. One can see how the time of flight does not substantially decrease,

Functional Requirements	Specification	Type
Position foot at pitch angle	Repositioning within step time 0.3s, Accuracy ±2°, move through water resistance, *(Without splashing too much), within smaller step times*	D *W*
Return foot roll to center and hold	Within duration 0.3s, Pre-loaded at zero position	D
Comply around pitch	Angle range ± 40°, Complies when external torque applied (ground contact), *Angle range ± 60°*	D *W*
Comply around roll	Angle range ±30°, Complies when external torque applied (ground contact)	D
Withstand operational loads	Carry weight 0.12kg of foot, endure acceleration forces of 3g	D
Robustness	The ankle does not suffer damage that prevents its functionality after any fall from TBD heights, *Verification with 2 TBD heights and masses at different r, p angles (0,5,10,20,40) on iron, mud, sand(TBD)*	D
Minimum lifetime	Withstand 10^6 cycles, (under fatigue limit, materials don't deteriorate, sun)	D
Water and dust proofing	IP67, no rust	D
Withstand Environment Temperatures	0 to 30°C, *-10 to 40°C*	D *W*
Determine foot pitch angle	Accuracy, resolution, frequency sufficient for positioning	D
Determine foot roll angle	Same as pitch	D
Foot Data and power pass-through	Cables from IMU	D
Performance Requirements		
Inertia minimization	Pitch inertia of entire foot <=0.02 kg m2	D
Weight minimization	Entire foot mass <= 400g	D
Design Requirements		
Size and Positioning	Fit on existing joint/foot/leg, No collision with ANYmal *Fit inside leg*	D *W*
Kinematics	No singularities in range of motion	D
Cabling	No cables stick out	D
Assembly	Can be assembled	D
Manufacturing	Can be manufactured	D
Heat emission	No interference with sensing, electronics etc., No damage to materials	D

Figure 3.5: List of Requirements for the actuated ankle: Sorted by requirement type, the degree to which they should be fulfilled is listed. "D" stands for demand and "W" for wish.

but that more notably the angular range covered by the shank increases.
Additionally, a ROS bag containing logging data from ANYmal walking was used to determine the step time. The estimated z-position of the contact points was plotted over time in rqt-multiplot for feet numbered 0 to 3. This corresponds to the vertical position of all four feet. The first of these plots is shown in Fig. 3.9(a). One can see how at each step the z position rapidly increases and then returns back to a similar value. The lift and land times at which these peaks in the graph start and stop were then measured from the plots by hand and tabulated in Fig. 3.9(b). Subsequently, the step times and their averages could be calculated. Furthermore, the smallest step times are highlighted and lie around 0.33 seconds, thus corroborating the measurements from the videos.
In terms of positioning accuracy, the requirements are not that high. For one, during flight a slightly mispositioned foot will not cause collisions in most cases. Second, once near to the ground before landing, a position offset will automatically be corrected once ANYmal puts its weight on the foot and the passive movement takes over. This was tested roughly by hand, and one found that an error of about

Sound emission	Bearable to the ear	D
Cost	Maximum cost of one foot considering a series of 100 pieces per year = 2500 Euros	W
Safety	No harm to person or property, *no pinching*	D *W*
Power consumption	<=75W	D
Efficiency	As high as possible	W
Jamming resistance	No jamming by stray objects	W
Modularity	As high as possible	W
Reparability	As high as possible	W
Modeling	As simple as possible	W
Control	As simple as possible	W
Complexity	As simple as possible, low part count	W
Interfaces		
Voltage and Power supply	48V up to 300 W	
Electrical Interface	USB max. power 500mA (fit-PC, max 1.5 A total), 2.4 A (Hub active port USB3)	
Signal	No analog signal routing to the body, check of signal integrity at interface to high-level control	
Connection to leg	Foot has to fit on interface of ANYmal (anydrive 1.2/2.1), Should be easily removable	
Connection to foot	To existing foot	
Connection to passive joint	To existing joint	

Figure 3.6: List of Requirements (continued)

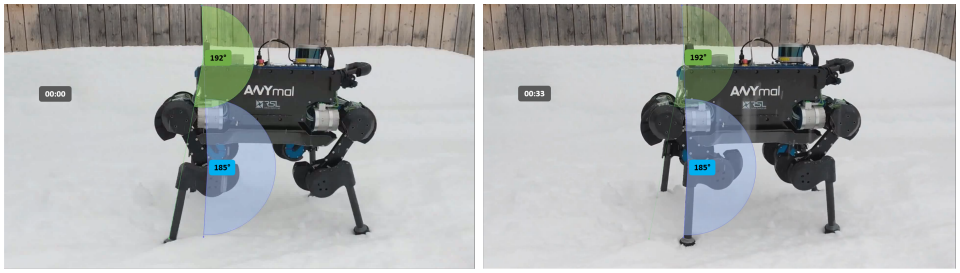

(a) Lift off

(b) Touch down after 0.33 seconds and 7° of shank movement

Figure 3.7: Video analysis in Kinovea: ANYmal walking at a typical speed, where the time is noted in grey and the start and end angles of the shank in colored boxes

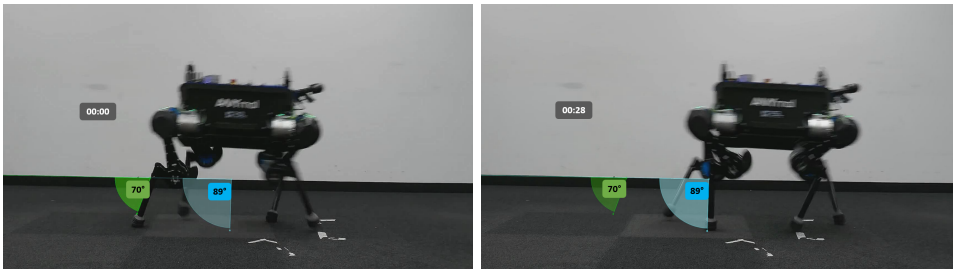

(a) Lift off

(b) Touch down after 0.28 seconds and 19° of shank movement

Figure 3.8: Video analysis in Kinovea: ANYmal walking at a high speed, where the time is noted in grey and the start and end angles of the shank in colored boxes

2° could still easily be compensated and in practice even larger angles would still be fine.
As for the roll movement, the ankle should be preloaded at its center position, so that it stays there even when the shank wobbles or moves. Only when in contact

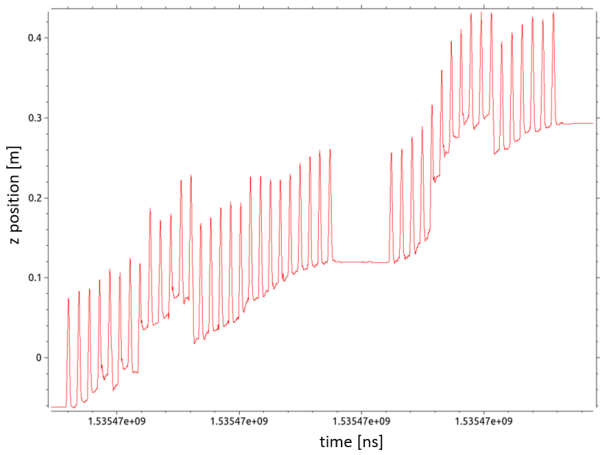

(a) Plot of the vertical z-position of foot number 0 over time

Foot nr.0

lift time	land time	delta t [s]
566.36	566.8	0.44
535.78	536.26	0.48
536.68	537.13	0.45
7.55	7.98	0.43
8.38	8.76	0.38
9.19	9.73	0.54
0.02	0.44	0.42
0.85	1.33	0.48
1.67	2.01	0.34
2.5	2.98	0.48
3.31	3.7	0.39
4.18	4.56	0.38
5.03	5.45	0.42
5.82	6.31	0.49
6.6	7.08	0.48
3.17	3.54	0.37
4.72	5.16	0.44
5.62	5.96	0.34
6.38	6.8	0.42
7.2	7.68	0.48
2.21	2.67	0.46
3.06	3.52	0.46
5.52	5.92	0.4
69.54	70.03	0.49
2.91	3.4	0.49
4.6	5.09	0.49
Average		0.44

Foot nr.1

lift time	land time	delta t [s]
8.79	9.26	0.47
39.61	40.02	0.41
7.07	7.51	0.44
7.85	8.23	0.38
1.11	1.51	0.4
6.78	7.21	0.43
5.11	5.53	0.42
2.5	2.89	0.39
5.04	5.52	0.48
Average		0.42

Foot nr.2

lift time	land time	delta t [s]
6.25	6.67	0.42
1.23	1.66	0.43
5.46	5.78	0.32
7.07	7.55	0.48
0.32	0.67	0.35
5.15	5.59	0.44
3.49	3.85	0.36
9.19	9.52	0.33
1.67	2.1	0.43
Average		0.40

Foot nr.3

lift time	land time	delta t [s]
7.54	8.01	0.47
5.03	5.43	0.4
9.07	9.47	0.4
4.79	5.2	0.41
6.36	6.77	0.41
2.18	2.67	0.49
6.38	6.77	0.39
7.13	7.52	0.39
3.77	4.16	0.39
Average		0.42

(b) Table of step time measurements from the plots of all four feet: Smallest step times and averages highlighted in green

Figure 3.9: Analysis of rosbag logging data

with the ground should the ankle give way and passively follow the leg's movement. Then when released it should automatically return to its initial position, as is the case with the passive ankle.
The pitch and roll range requirements are set by the THING project, with a larger range for pitch, the more important rotation when walking.

3.4 Other Requirements

Then there are the physical robustness requirements, one of which is that the ankle should be able to withstand falls without damage. This should be verified with a fall test machine available in the lab. During its lifetime it should also hold up after one million movement cycles and be water and dust proof. This waterproofing requirement is not critical in this project and could be loosened, because for the production version of the ankle others will finalize this.
Two key requirements affect the performance of the ankle. The inertia and mass of the foot influence how much torque is required to accelerate the foot, so both should be kept as low as possible.

Various desirable features of the ankle are listed in the design requirements, for instance a system that fits inside the existing leg and could easily be slid out for modifications would be ideal. At the same time a simple system is strived for, since that keeps the number of parts, cost, and number of potential problem areas down.

3.5 Requirement Weights

Next, all 20 requirements were given individual weights in Figure 3.10 to later use in a use value analysis. They are sorted into positioning requirements for roll and pitch, durability, mounting, performance and design requirements. Each of these categories except mounting has a sum weight of eight or nine, since they are all essential and would not make a functional solution without each other. For some requirements, possible metrics by which to grade how much a concept fulfills that requirement are listed. In order to then grade the concepts, a simple symmetrical five-tier grade system shown in Figure 3.10 was used.

	Requirement	Possible metric	Weight	
1	**Pitch Positioning speed**	lever arm, transmission type	1	
2	**Pitch Positioning Accuracy**	friction, play	1	
3	**Pitch Range of motion**	limited or not?	1	
4	**Pitch rolling compliance**	controlled by motor	1	
	Pitch Positioning Requirements			**Σ4**
5	**Passive return to center speed**		1	
6	**Passive hold strength**		1	
7	**Roll Range of motion**		1	
8	**Roll rolling compliance**		1	
	Roll Positioning Requirements			**Σ4**
	Positioning Requirements			**Σ8**
9	**Ability to withstand operational loads**		2	6
10	**Impact robustness**	thick parts, few parts, few connections	2	
11	**Lifetime**	Wear, deteriorating materials, friction	2	
	Mechanical Durability Reqs.			**Σ6**
12	**Ease of waterproofing**	Exposed compenents, compenents sensitive to water	1	
13	**Temperature resistance**	temperature sensitive components	1	
	Environmental Durability Reqs.			**Σ2**
	Durability Requirements			**Σ8**
14	**Ease of measuring ankle position, velocity**	mounting points	1	
15	**Space for cables to passthrough**	size around ankle, shank	1	
	Mounting Requirements			**Σ2**
16	**Small overall Inertia**	mass close to knee joint	4	
17	**Low weight**	mass	4	
	Performance Requirements			**Σ8**
18	**Small size, low profile, integration into leg**		4	
19	**Modularity, Repairability**		1	
20	**Complexity**	No. of parts and joints	4	
	Design Requirements			**Σ9**
	Total			**Σ35**

Grade		Meaning
5	++	Very good
4	+	Good
3	0	Neutral
2	-	bad
1	--	very bad

Figure 3.10: Requirement weights and grading table

Chapter 4

Conceptual Design

After defining the requirements and their individual importance in the last section, one could now try to generate concepts that meet the requirements well. For this a use value analysis was performed, where concepts are generated from subfunctions in a morphological box and graded on the weighted requirements.

4.1 Morphological Box

In the morphological box in Figure 4.1 the system was divided into necessary functions. First, the overall actuation mechanism, defining the general position an type of movement of the actuator and how the movement is brought to the joint. Second, the type of actuator (which may include reduction gears) followed by the transmission. Lastly, spring and damping systems for pitch and roll are listed. For each of the functions as many solutions as possible were entered, many of which can be found in the existing ankles found in the literature research (section 2.2).

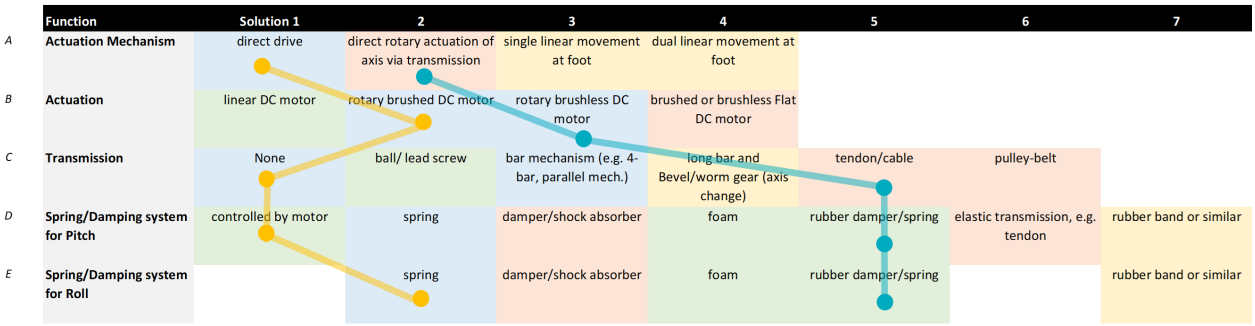

Figure 4.1: Morphological box: System functions and solutions. Cells are colored for easier legibility and in most cases adjacent equally colored cells contain similar or the same solutions.

Then all possible combinations of different solutions for each function were considered and all physically possible ones tabulated in Figure 4.2. For example concept 1 is directly driven by using a rotary motor inside its joint without any transmission. The last two functions D and E are largely independent of the first three A-C, which is why no specific one is listed yet, except where natural (tendon/cable transmission D4-5). Thus they can be looked at later, once a concept with the first three functions has been chosen. This resulted in a total of 13 different concepts, which are grouped first by actuation mechanism and then further distinguish each other going down the rest of the table.

	Function	Concept 1	2	3	4	5	6	7	8	9	10	11	12	13
A	Actuation Mechanism	direct drive		direct rotary actuation of axis via transmission			single linear movement at foot			dual linear movement at foot				
B	Actuation	rotary brushed or brushless DC motor	flat motor	rotary brushed or brushless DC motor			linear DC motor	rotary brushed or brushless DC motor		linear DC motor		rotary brushed or brushless DC motor		
C	Transmission	none	none	bevel/worm (w/ axis change)	tendon/cable	pulley-belt	bar mechanism	ball/ lead screw	bar mechanism	bar mechanism	tendon/cable	ball/ lead screw	bar mechanism	tendon/cable
D	Spring/Damping system for Pitch	any except elastic transmission	any except elastic transmission	any except elastic transmission	elastic transmission or any other	elastic transmission or any other	any except elastic transmission	any except elastic transmission	any except elastic transmission	any except elastic transmission	elastic transmission or any other	any except elastic transmission	any except elastic transmission	elastic transmission or any other
E	Spring/Damping system for Roll	any	any	any	any	any	any	any	any	any	any	any	any	any

Figure 4.2: Concepts generated with the morphological box: Each concept consists of a specific set of solutions for each function.

4.2 Use Value Analysis

Next, all of these 13 concepts were evaluated in a use value analysis (Fig. 4.3), where each was given grades for how well it fulfills each requirement. Then each grade was multiplied by the requirement weight, so that a weighted average grade could be calculated for every concept. For most of the pitch positioning requirements no grade was given, since that would depend on the spring/damping system, which as mentioned previously would be selected afterwards.

	Requirement	Possible metric	Weight	Concept 1	2	3	4	5	6	7	8	9	10	11	12	13
1	Pitch Positioning speed	lever arm, transmission type	1	4	4	3	3	3	3	2	3	3	3	2	3	3
2	Pitch Positioning Accuracy	friction, play	1	4	4	3	2	2	3	3	3	3	2	3	3	2
3	Pitch Range of motion	limited or not?	1	5	5	5	5	5	1	2	2	1	1	2	2	2
4	Pitch rolling compliance	controlled by motor	1	3	3	3	3	3	3	3	3	3	3	3	3	3
	Pitch Positioning Requirements		Σ4													
5	Passive return to center speed		1													
6	Passive hold strength		1													
7	Roll Range of motion	something in the way of roll	1	1	1	5	5	5	2	2	2	2	2	2	2	2
8	Roll rolling compliance		1													
	Roll Positioning Requirements		Σ4													
	Positioning Requirements		Σ8													
9	Ability to withstand operational loads		2	3	3	3	3	3	3	3	3	3	3	3	3	3
10	Impact robustness	thick parts, few parts, few connections	2	4	4	3	2	2	3	3	3	2	2	2	2	2
11	Lifetime	Wear, deteriorating materials, friction	2	4	4	3	2	2	3	2	3	3	1	2	3	1
	Mechanical Durability Reqs.		Σ6													
12	Ease of waterproofing	Exposed compenents, compenents sensitive to water, no. of compants.	1	4	4	3	3	3	3	3	3	2	2	2	2	2
13	Temperature resistance	temperature sensitive components	1	3	3	3	2	2	3	3	3	3	2	3	2	3
	Environmental Durability Reqs.		Σ2													
	Durability Requirements		Σ8													
14	Ease of measuring ankle position, velocity	mounting points	1	5	5	4	4	4	5	5	5	5	5	5	5	5
15	Space for cables to passthrough	size around ankle, shank	1	4	4	4	5	5	4	4	4	3	3	3	3	3
	Mounting Requirements		Σ2													
16	Small overall Inertia	mass close to knee joint	4	1	1	4	5	5	3	3	3	2	4	2	2	4
17	Low weight	mass, heavy transmission, suprt struct.	4	5	5	3	4	4	2	3	3	1	2	1	1	2
	Performance Requirements		Σ8													
18	Small size, low profile, integration into leg		4	1	2	5	5	4	2	3	2	1	1	1	1	1
19	Modularity, Repairability		1	5	5	4	3	3	3	2	3	2	1	1	2	1
20	Complexity	No. of parts and joints	4	5	5	4	3	3	3	2	3	1	1	1	1	1
	Design Requirements		Σ9													
	Total		Σ35	61	62	62	59	58	49	48	51	40	38	38	40	40
	Weighted Average Grade			3.09	3.20	3.40	3.34	3.23	2.51	2.54	2.66	1.80	1.94	1.71	1.80	2.00

Figure 4.3: Use value analysis

For example, concept 1 received a low roll range of motion score (R7: Requirement 7), because a long motor inside the ankle joint and a wide joint assembly would stand in the way of roll movements. It also shows weakness in its overall inertia (R16) and integration (R18). Concept 2 gets the same grades, except for better integration (R18) due to the flat motor form factor.
The third concept receives a high grade for R7, because the motor is moved away from the joint by a transmission. It also scores higher on integration because the motor could be housed inside the leg. The next two concepts 4 and 5 receive overall

similar scores because of the similarity of their tendon and belt transmissions. They most notably reduce the inertia R16 by moving the motor close to the knee and are suited for integration inside the shank (R18).
Concepts 6 through 8 involve creating a linear movement at the foot. For this a linear motor is used in concept 6, however this motor is naturally limited by its rod length, opposed to rotary motors that can spin without limit. This gives it a low R3 grade. The tendon transmission of concept 7 gives it a low complexity and modularity score (R19,20).
The last concepts 9 to 13 all involve dual linear movements at the foot. Concepts 9 and 11 are simply concepts 6 and 7 with twice the actuators and transmission, whereas concept 12 uses double the transmission and optionally double actuators. Due to their increased part count, they perform poorer compared to their counterparts on complexity, the other design requirements and weight.
The remaining two concepts 10 and 13 use tendons or cables that can only transmit pulling forces. By attaching the tendons on opposite ends of the foot, the tendons can pull on either side and rotate in both directions. Again the complexity of the tendon system leads to poor scores in that area.
The resulting use value for each concept shows similar numbers for concepts 1 through 5 (∼3.2) and lower scores(∼2.5) for concepts 6 to 8. The remaining ones are dual concepts with scores of 2 or below. This shows that the dual concepts result in no significant benefit over their single movement counterparts, while still increasing complexity and weight.
One then decided to pursue one most promising concept of each of the remaining actuation method groups (concepts 1-2, 3-5, 6-8), because they all scored in a similar range and were still all viable candidates. Of the direct drive mechanism, one chose to keep both concepts 1 and 2, because they are the same concept, only with a differently shaped motor.

4.3 Motor Sizing

The selected concepts were then investigated further and in more detail, so that they could be compared more concretely. In order to create such higher resolution concepts, first a sample of their main component, their motor, was selected.

4.3.1 Simple Model

The requirements for such a motor were estimated using simple calculations, with the ankle model in Fig. 4.4. Here the ankle joint is connected to the foot with mass m at a distance s. We assume the shank and the rest of ANYmal are static for this case. In equilibrium state a torque T_{jnt} must be applied at the joint, which is provided by a motor after any eventual transmission. This torque compensates gravity acting on the foot. The required torque is greatest at $\phi = 90°$, where none of the gravity load is taken by the joint.

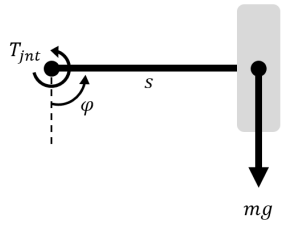

Figure 4.4: Simple ankle model at $\phi = 90°$ and in equilibrium

One wanted to determine the minimum required torque of a motor, because generally small rotary electric motors have low torque and require a transmission. So torque is generally the bottleneck. With a low torque requirement a transmission could potentially be avoided and a motor that is as small and light as possible can be chosen. To represent the required movement from one end to the other a trapezoidal angular velocity profile was used (Fig. 4.5). Then the question was, which t_1 leads to the lowest torque. We can see that $t_1 = T/2$, resulting in a triangular profile leads to low acceleration and therefore low torque.

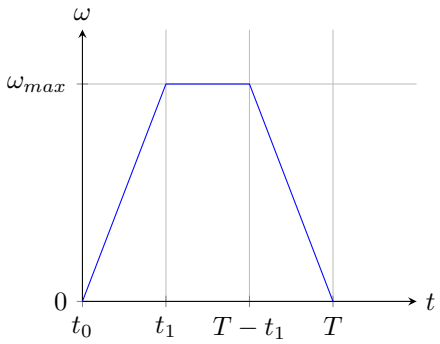

Figure 4.5: Trapezoidal velocity profile

We can also show this mathematically and compute the required power by determining w_{max}:

$$\begin{aligned}\phi_{tot} &= \frac{t_1 w_{max}}{2} 2 + w_{max}(T - t_1 - t_1) \\ &= t_1 w_{max} + w_{max}(T - 2t_1) \\ &= w_{max}(T - t_1) \\ w_{max} &= \frac{\phi_{tot}}{T - t_1}\end{aligned}$$

Writing a torque equilibrium:

$$\begin{aligned}T_{motor} &= T_g + T_{acc} \\ &= mgs + I\dot{w} = mgs + I\frac{\omega_{max}}{t_1} \\ T_{motor}(t_1) &= mgs + I\frac{\phi_{tot}}{(T - t_1)t_1}\end{aligned}$$

From which the power can also be obtained:

$$\begin{aligned}P_{motor} &= T_{motor} \cdot \omega_{max} \\ P_{motor}(t_1) &= mgs\frac{\phi_{tot}}{T - t_1} + \frac{I}{t_1}(\frac{\phi_{tot}}{T - t_1})^2\end{aligned}$$

We can look at the edge cases of t_1 affecting the torque:

$$\text{for } t_1 = \frac{T}{2} : P_{motor}\Big(\frac{T}{2}\Big) = 2mgs\frac{\phi_{tot}}{T} + 2\frac{I}{T}\Big(\frac{2\phi_{tot}}{T}\Big)^2$$
$$= 2mgs\frac{\phi_{tot}}{T} + 8I\frac{\phi_{tot}}{T^3}$$
$$\text{for } t_1 \to 0 : P_{motor}(0) = mgs\frac{\phi_{tot}}{T} + \infty = \infty$$

And find the minimum of T_{motor}:

$$\frac{d}{dt_1}T_{motor}(t_1) = \frac{d}{dt_1}(I\phi_{tot}t_1^{-1}(T-t_1)^{-1})$$
$$= I\phi_{tot}\Big[-t_1^{-2}(T-t_1)^{-1} + t_1^{-1}(T-t_1)^{-2}\Big]$$
$$= I\phi_{tot}\Big[-\frac{1}{t_1^2(T-t_1)} + \frac{1}{t_1(T-t_1)^2}\Big] \stackrel{!}{=} 0$$
$$\frac{1}{t_1(T-t_1)^2} = \frac{1}{t_1^2(T-t_1)}$$
$$\frac{1}{T-t_1} = \frac{1}{t_1}$$
$$t_1 = T - t_1$$
$$t_1 = \frac{T}{2}$$

Which is indeed the edge case $T/2$, leading to the triangular profile in Fig. 4.6.

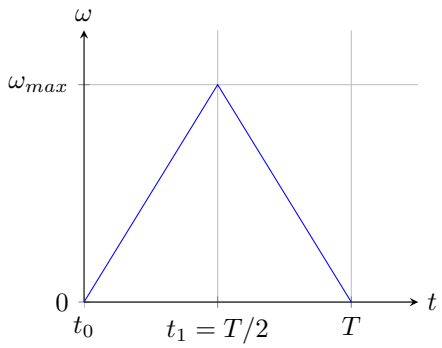

Figure 4.6: Triangular velocity profile

Using the following rough values, P_{motor} and T_{motor} could be estimated (using the MATLAB script motorEstimation.m):

$$m = 0.12kg$$
$$\phi_{tot} = 80°$$
$$T = 0.3s$$
$$s = 0.04m$$
$$I = 0.000192kgm^2$$
$$T_{motor}(t_1 = T/2) = 59mNm$$
$$P_{motor}(t_1 = T/2) = 0.55W$$

4.3.2 Detailed Model

Next, a more detailed double pendulum model was used to determine the equations of motion of the ankle. The model in Fig. 4.7 and EOM were taken from [18] where the foot was then represented by link 2 and the ankle joint by joint 2. Both the shank and thigh were combined and approximated by the single link 1, because what matters most to the ankle is the resulting movement at the ankle joint, and not what happens within the leg.

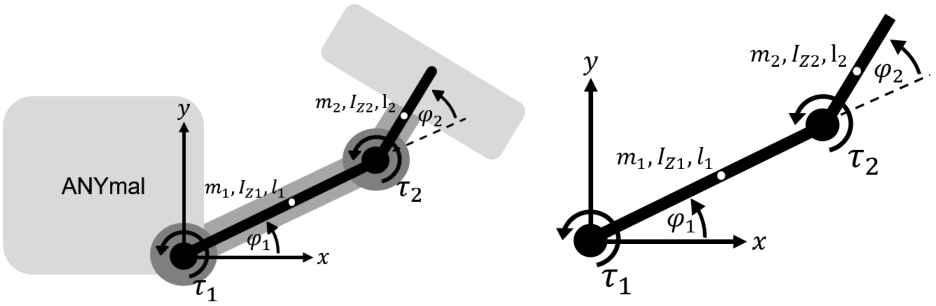

(a) Simplified ANYmal sketch (b) Double pendulum

Figure 4.7: Leg and foot as double pendulum.

The EOM in (4.1) allows one to calculate the required ankle torque τ_2:

$$\begin{bmatrix} \alpha + 2\beta\cos\theta_2 & \delta + \beta\cos\theta_2 \\ \delta + \beta\cos\theta_2 & \delta \end{bmatrix} \begin{bmatrix} \ddot{\theta}_1 \\ \ddot{\theta}_2 \end{bmatrix} + \begin{bmatrix} -\beta\sin\theta_2\dot{\theta}_2 + b_1 & -\beta\sin\theta_2(\dot{\theta}_1 + \dot{\theta}_2) \\ \beta\sin\theta_2\dot{\theta}_1 & b_2 \end{bmatrix} \begin{bmatrix} \dot{\theta}_1 \\ \dot{\theta}_2 \end{bmatrix} + \begin{bmatrix} m_1 g r_1 \cos\theta_1 + m_2 g(l_1\cos\theta_1 + 2r_2\cos\theta_1) \\ m_2 g r_2 \cos(\theta_1 + \theta_2) \end{bmatrix} = \begin{bmatrix} \tau_1 \\ \tau_2 \end{bmatrix} \tag{4.1}$$

where

$$\begin{aligned} \alpha &= I_{Z1} + I_{Z2} + m_1 r_1^2 + m_2(l_1^2 + r_2^2) \\ \beta &= m_2 l_1 r_2 \\ \delta &= I_{Z2} m_2 r_2^2 \\ I_{Zi} &= I \text{ of link } i \text{ w.r.t. to its C.O.G. and to the } z\text{-axis} \end{aligned}$$

Before that, the inertia moment of the foot was calculated based on the CAD model's dimensions and by approximating the foot as a solid block with width b and height h:

$$\begin{aligned} m &= 0.12kg \\ b &= 100mm \\ h &= 35mm \\ d_{COG-axis} &= \sqrt{(9mm)^2 + (7.5mm)^2} = 11.75mm \\ I_{Z,COG} &= \frac{1}{12} m(b+h)^2 \\ I_{Z,axis} &= I_{Z,COG} + m d_{COG-axis}^2 \\ &= \frac{1}{12} m(b+h)^2 + m d_{COG-axis}^2 = 1.29 \cdot 10^{-4} kgm^2 \end{aligned}$$

Because this yielded a lower value than the previous one provided from the start, the higher one was used from here on to be on the safe side. Initially, the values

calculated with the EOM were unreasonable, which is why a simpler model was created to double check the equations. In this model in Figure 4.8 torque is only applied to the ankle joint.

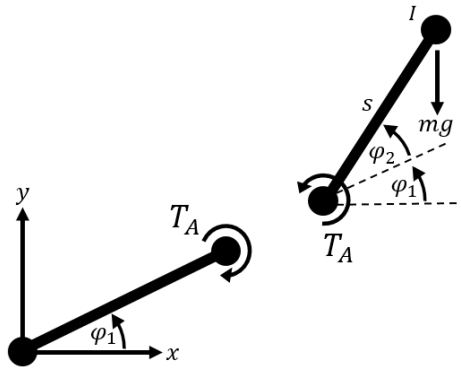

Figure 4.8: Free cut of simple leg and foot model

By doing a free cut and subsequent angular momentum balance an expression for the torque was obtained:

$$I\ddot{\phi}_2 = T_A - mgs\cos(\phi_1 + \phi_2) \tag{4.2}$$

$$T_A = I\ddot{\phi}_2 + mgs\cos(\phi_1 + \phi_2) \tag{4.3}$$

Comparing (4.3) and the EOM in (4.1) a typo in the source paper was found, that had lead to the incorrect values. In their cosine shorthand notation, c_{12} was misspelled as c_12. With the corrected EOM the values could be calculated with a MATLAB script (TorqueFromEOMwithLegAcc.m) using:

$$\begin{aligned} m_2 &= 0.12kg & l_1 &= 0.299m \\ r_2 &= 0.0075m & b_1 &= b_2 = 0 \\ I_{Z2} &= 0.000192kgm^2 & \phi_{tot} &= 80^\circ \\ \phi_{tot,leg} &= 7^\circ & T &= 0.3s \\ \phi_1 &= -102^\circ & \phi_2 &= -40^\circ \end{aligned}$$

one obtains

$$\begin{aligned} \dot{\phi}_{2,max} &= 88.9rpm \\ \tau_2 &= 17.2mNm \\ P_2 &= 0.16W \end{aligned}$$

And a safety factor of 3 on $T = 0.1s$ resulted in:

$$\begin{aligned} \dot{\phi}_{2,max} &= 267rpm \\ \tau_2 &= 105mNm \\ P_2 &= 2.92W \end{aligned}$$

In order to determine the continuous torque requirement for the motor, the root

mean square (RMS) torque was calculated [19]:

$$\begin{aligned} T_{acc} &= T_{dec} = 105mNm \\ t_{acc} &= t_{dec} = 0.05s \\ t_{run} &= 0 \\ t_{idle} &= 0.2s \\ T_{RMS} &= \sqrt{\frac{T_{acc}^2 t_{acc} + T_{run}^2 t_{run} + T_{dec}^2 t_{dec}}{t_{acc} + t_{run} + t_{dec} + t_{idle}}} = 60.6mNm \end{aligned}$$

To select a linear motor, the required force and velocity were computed:

$$\begin{aligned} a &= 45mm \\ F &= \frac{\tau_2}{a} = 2.33N \\ v &= \omega a = \dot{\phi}_{2,max} a = 1.35m/s \\ a &= \dot{\omega} a = 25.1m/s^2 \end{aligned}$$

Again the continuous force requirement was determined:

$$\begin{aligned} F_{acc} = F_{dec} &= 2.33N \\ F_{idle} &= mg = 0.19kg * 9.81m/s^2 = 1.86N \\ t_{acc} = t_{dec} = t_{idle} &= 0.0333s \\ F_{RMS} &= \sqrt{\frac{2F_{acc}^2 t_{acc} + F_{idle}^2 t_{idle}}{t_{acc} + t_{dec} + t_{idle}}} = 1.55N \end{aligned}$$

4.3.3 Candidate Motors

Then a search for motors meeting these requirements was conducted, by considering motors of the same make that had been used in other existing ankles along with any other commercially available ones. The resulting motors and in some cases accompanying gear trains for each concept are listed in Fig. 4.9. The Maxon motors were found by both searching through their catalog and double checking by using their selection program.

4.4 Preliminary Design

Next, simple CAD mockups of the concepts could be created using the selected motors.

4.4.1 Direct Drive Concepts

Fig. 4.10 shows the concept with a motor directly embedded inside the ankle joint. The model represents the main dimensions of the existing passive ankle alongside manufacturer CAD-models of the motor and gearhead, surrounded by a provisional bearing. One can see how the ankle joint would have to be completely redesigned and enlarged to house the motor. This would make the ankle quite a complicated assembly. It would at the same time have to transfer the forces of the mass of ANYmal around the motor as connecting the output rod of the motor to the foot

Concept	Direct Drive		Linear	Tendon
Motor Specs	**1**	**2**	**3**	**4**
Brand	Maxon	Maxon	Faulhaber	
Name	EC 13, 430164, with Hall Sensors	EC 45, 339282, with Hall Sensors	Linear DC-Servomotor with Analog Hall Sensors, LM 1247 040 11	same as 1
Linear or Rotary	R	R	L	
Type	brushless DC	flat brushless DC	DC servo	
max cont T/F	5.38mNm	66 mNm	3.6N	
Idle speed	26'600rpm	4750rpm	2.4m/s	
Acceleration			148.5 m/s2	
Power	12W	30W	36W elec., 8.64W mech.	
max F/T			10.7N	
range of motion			40mm	
diameter/width	13mm	45mm	12.5x19mm	
length	33.5mm	19.7mm	49.4mm	
Mass	29g	75g	63g	
Voltage	36V	36V	under 75V	
Temp. range	-40 to 100°C		-20 to 125°C	
Lifetime			multiple million cycles	
Price	216 €	73 €	219.5 CHF	
Availabilty	2 wks	to be manufactured	from stock or 4-5 wks	
Fitting Gear	**1**	**2**	**3**	**4**
Brand	Maxon	without	without	
Name	Planetary Gearhead GP 13, 110314			
Linear or Rotary	R			
Type	Planetary			
Reduction ratio	17:1			
Max. Efficiency	83%			
diameter/width	13mm			
length	19.9mm			
Mass	14g			
Temp. range	-15...+100 °C			
Price	47			
Availabilty	2 wks			
Total mass	43g	75g	63g	43g

Figure 4.9: Possible components for the remaining candidate concepts (datasheets in appendix B)

and allowing rotation about two axes. Furthermore, at the current configuration, the width of the motor-gear combination would prohibit any roll movement. So the joint would have to be placed a lot higher, which would make the leg more susceptible to ankle twisting as occurs in humans. This because already a much smaller roll movement of the ankle would lead the vector of force coming through the shank to point outside of the sole.

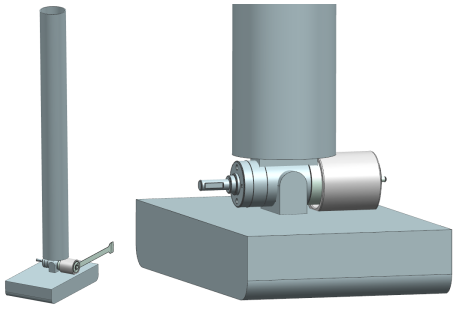

(a) Overview (b) Close-up view

Figure 4.10: Direct drive concept CAD-mockup. The cable of the motor is what extends from it rigidly to the back and will change later.

The second concept using the flat motor is depicted in Fig. 4.11, where the motor

can be placed out of center of the joint, due to its flatness. Due to it's large size no gearhead is need, however it's large diameter requires a taller joint again. Here the motor is fixed to the upper fork, through which the rotating shaft extends and is connected to the intermediate cube. Again, this would lead to a more complicated joint design.

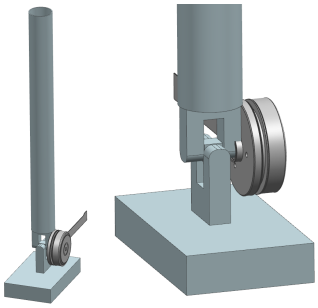

(a) Overview (b) Close-up view

Figure 4.11: Flat direct drive concept CAD-mockup

4.4.2 Tendon Driven Concept

The tendon driven mockup in Fig. 4.12 again uses the same brushless motor and gearhead as the first concept. This time however, they are positioned vertically inside the shank and drive a disk to which tendons are fixed. These are redirected downward by further discs, exit the shank and pull on a corresponding disk at the joint. This disk is attached to the axle that goes through the upper fork and is affixed and rotates with the intermediate cube. The redirecting disks would be spring loaded, so as to keep the tendons taught at all times. Additionally, small contactless magnetic angle sensors are shown at the joint. These use a small cylindrical permanent magnet along with a sensor that measures the rotation of this magnet. Here the magnet is attached to the rotating axle and the sensor would be mounted to the correspondingly not rotating fork. In this way, the pitch and roll angles could each be directly measured. Later one however opted to use the already embedded IMU's in both sole and shank to obtain these values.
This concept has the advantage that most of the power train is housed inside the shank, protecting it against any impacts and sealing it off from water and dust. At the same time this complicates the mounting and assembly of the motor due to difficult access to the inside. The tendons' transmission mechanism allows the heavy motor to be placed high up in the shank, decreasing the overall assembly's inertia with respect to the knee joint. On the other hand, the mechanism adds complexity and friction on the disks. Furthermore, the tendons could slip off the disks and have some slack when changing directions. Since they are flexible, their slight elongation might adder further inaccuracies. And the tensioning springs have to be selected just right, as to be tight enough to avoid slack, but not overly tight to increase the friction.

4.4.3 Linear Drive Concept

Lastly, the concept in Fig. 4.13 uses a linear motor without any gears or ball screw to actuate the ankle. It is mounted outside along the shaft and connected via a rod

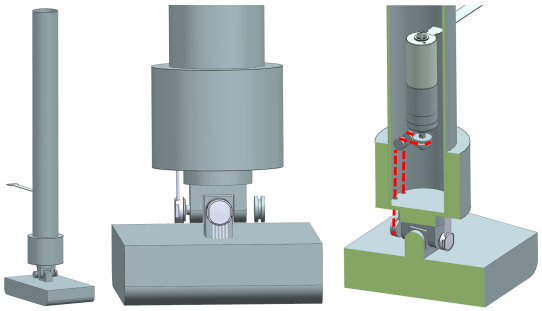

(a) Overview (b) Close-up view (c) Section view

Figure 4.12: Tendon driven concept CAD-mockup

to the foot. At both connecting ends of the rod there are universal joints, to allow simultaneous pitch and roll movement.
This concept has the advantage of being relatively simple, requiring no modification to the ankle joint itself and only small changes to the rest. Additionally, the mounting space for the motor is much less constrained, unlike in the concepts where the motor is inside the joint or shank. Potentially the linear motor could also be housed inside the shank, though this would require a long opening along its height as well a bearing guided arm reaching out of the shank. Here jamming could be an issue, the overall complexity would increase and the shank would be weakened.
This particular motor is directly driven, which avoids any issues gears would bring. There is no play when changing directions, no transmission losses and it is backdrivable, which avoids damage when the joint is suddenly moved in an impact. The motor's long shaft means it requires quite a lot of space, however that is not an issue, since the motor's form factor nicely matches with the shank.
The rod mechanism connecting motor to foot is also rigid, which allows the foot to be accurately positioned. In this concept however, the motor and rod are quite exposed and may be at risk of impact with the surroundings.

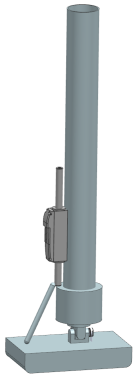

Figure 4.13: Linear motor concept CAD-mockup

4.4.4 Concept Comparison

After comparing the remaining concepts in simple CAD models, one decided to continue pursuing the linear motor concept as well as the flat direct drive one with a slight modification. Instead of having the flat drive inside the joint, it would

be placed higher up outside the joint and would be connected to the foot with a rod in a similar manner as in the linear concept. This would allow the joint to remain largely unchanged and make an overall more simple and realizable system. Equally, the linear concept was kept on to have a simple concept without any major foreseeable issues in the implementation. It also has lower inertia, because its motor is placed higher up.
On the other hand, the first direct drive concept was discarded due to the complexity of the joint assembly and the fact that the joint would have to be moved higher up. Furthermore, the motor and gearhead assembly is too wide in comparison with the flat drive. The flat one's dimensions are also more suitable for the modified concept with the rod. The gearhead was also unwanted, since it might not be backdrivable, add inaccuracies, wear and could be an additional point of failure.
Similarly, the tendon driven concept was also ousted for using the same gearhead and being quite complex overall, which means issues could arise at many points. These points could be problematic during implementation, but are also points where things might break during use. In particular, it might be tricky to get the tensioning of the tendons just right, as well as making room for the tendons to pass through the entire force sensor.
The remaining two concepts were fleshed out even further in the next step, until with increasing design detail a superior concept would emerge.

4.4.5 Flat Direct Drive Ankle Version 1

The concept using the flat direct drive was remodeled in more detail based on the latest available existing passive ankle design. It also incorporates the modified motor placement and transmission mechanism (Fig. 4.14).

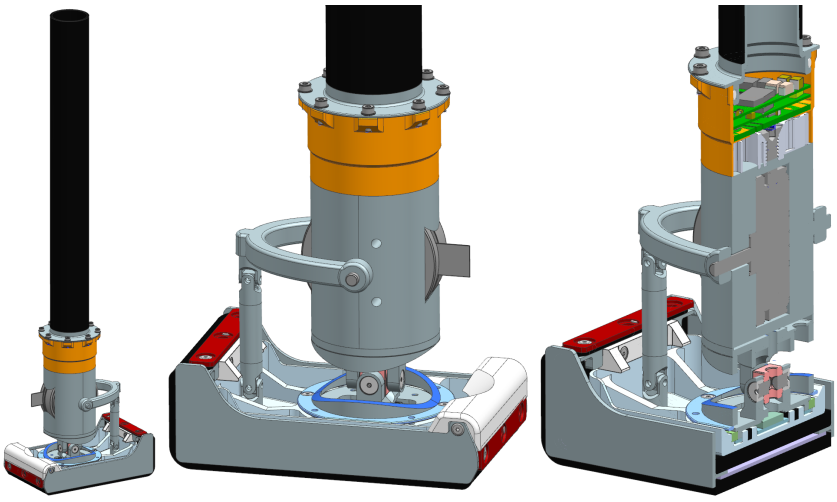

(a) Overview (b) Close-up view (c) Section view

Figure 4.14: Flat direct drive CAD model

Here the drive is housed in an added shank section between the force sensor and the upper fork. It is parted in two to allow the motor to be mounted inside using screws at mounting bores. Keeping this section the same diameter as its neighbouring parts, the motor only sticks out slightly, keeping a relatively compact design. On one side, the motor shaft passes through and is attached to a fork that is bearing-supported on a shaft on the opposite side. The fork has an elliptical shape, so that when maximally deflected, it aligns nicely with the shank's surface. That makes

it use the least amount of material necessary, keeping its weight down. It then connects to the foot over a pair of universal joints and a rod.
At the ankle joint, the rubber spring is replaced by one split in two with varying height along its circumference. Along the width of the foot, the height is highest, so that they make contact when pitching and function as the normal spring would. By changin the height one can adjust at which angle the damping starts. Correspondingly, the height is lowest along the foot's length, so that the springs do not contact at all and do not work against the motor. One could opt to have a bit of remaining height, so that there would be slight damping at the ends of the range of motion which would help dampen impacts. However, manufacturing the springs in such a shape might be problematic, as well as fixing them to the foot and shank. Furthermore, both rubber ends might slip off each other when pressed together, if not made wide enough.

4.4.6 Linear Ankle Version 1

Similarly, the linear motor concept was adapted to the passive ankle CAD (Fig. 4.15). A provisional mounting block attached to the carbon shank allows the motor to be attached. This at a height that allows enough clearance for the motor rod to be fully extended. It also increases the moment arm of the motor, the distance between the motor rod axis to the ankle joint axis. A connecting part screws on to the end of the rod and connects to the foot via universal joints and a rod. In this case two universal joints are necessary, because the lower one is not aligned with the ankle joint axis.

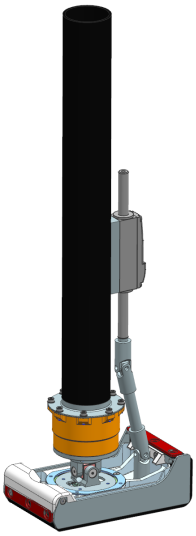

Figure 4.15: Linear motor CAD model

4.4.7 Choice of Concept

If one compares both concepts, one can see how the lower transmission part is largely the same, both have a rod and joints, only in the case of the flat drive there is an additional fork. However, the amount of material needed to mount the motor is much higher for the flat motor concept. In addition, the flat drive is also heavier at 75 grams opposed to the linear drive's 63, meaning that the overall system will be heavier. Also, the linear motor rod's weight is already included in the motor's weight, while the flat drive has an additional fork.

Most of the mass of the flat drive concept is also concentrated near the ankle joint, so that it has higher inertia with respect to the knee and hip joints. Opposed to the linear motor concept, where the motor is located higher up.
At the same time, the linear concept beats the rotary one in terms of complexity. The flat drive needs an additional bearing axle, whereas the bearings are already integrated inside the linear motor. The linear motor mounting is also far simpler, while the flat motor's housing has to fulfill many functions at the same time, like support the weight of the robot, connect to the force sensor and upper ankle joint fork, hold the motor and guide cables. It also has to hold together its two halves and provide a rotation axis for the elliptical fork.
The linear motor concept also allows very easy access to the motor from the outside and is very flexible for any modifications. The motor size and height position can easily be varied and its open access makes for fast and easy repairs. On the flipside, the flat motor is encased in multiple layers of parts and is more complex to assemble. And its housing is made specifically for one motor with less room for adjustments. The flat drive housing's many gaps would also make waterproofing along them more involved.
For all of these reasons the linear motor concept was ultimately chosen. It makes a much lighter, simpler and more flexible system.

Chapter 5

System Design

5.1 Bar Mechanism

5.1.1 Simple Model

For the linear mechanism, a simple kinematic model (Fig. 5.1) was analysed to see the influence of the motor positioning on the resulting torque. Here the ankle is in neutral position and gravity is not considered:

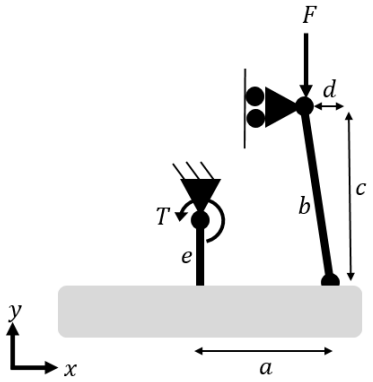

Figure 5.1: Linear concept kinematic model

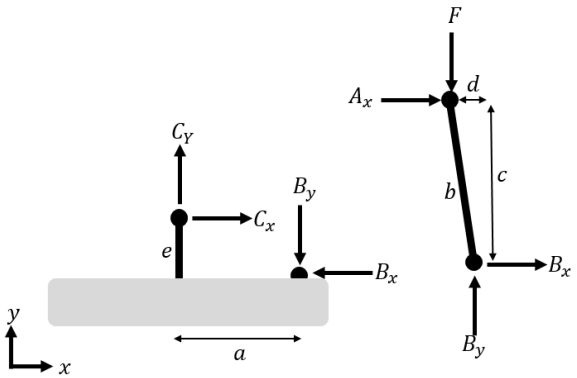

Figure 5.2: Free body diagram

A free body diagram (FBD) (Fig. 5.2) yields the equations:

$$
\begin{aligned}
B_y - F &= 0 \\
B_y d + B_x c &= 0 \\
-T - B_y a - B_x e &= 0 \\
B_x &= -B_y \frac{d}{c} = -F\frac{d}{c} \\
T &= -Fa + B_x e \\
T &= -Fa + F\frac{d}{c}e = F(\frac{de}{c} - a) \\
\text{if } c = 2e,\ T &= F(\frac{d}{2} - a)
\end{aligned}
$$

One can see how increasing d leads to a lower torque, so ideally d is as small as possible. A larger b also increases the amount of resulting torque.

5.1.2 Detailed Model

A more detailed model in Fig. 5.3 was made to see the effect of the ankle angle on the motor's displacement s and transmitted force. Here the mass of the foot is not included, because it was already accounted for in the calculations for the required ankle torque.

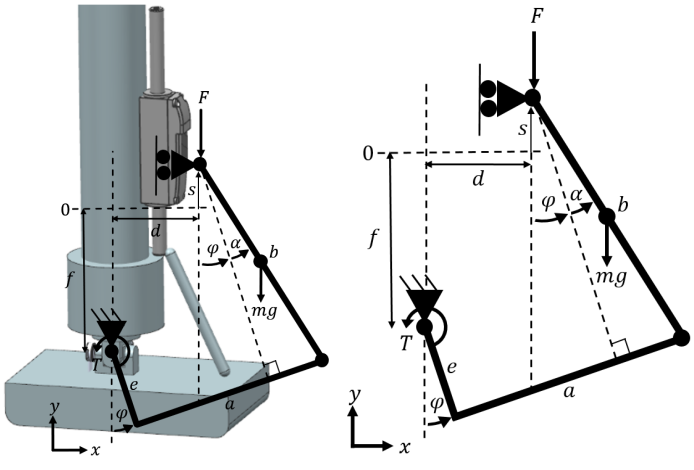

(a) Overlaid schematic (b) Linear mechanism

Figure 5.3: Linear concept kinematic model at angle ϕ

With the FBD in Fig. 5.4 and force and torque balances we get expressions for the torque T as a function of the force F and vice versa:

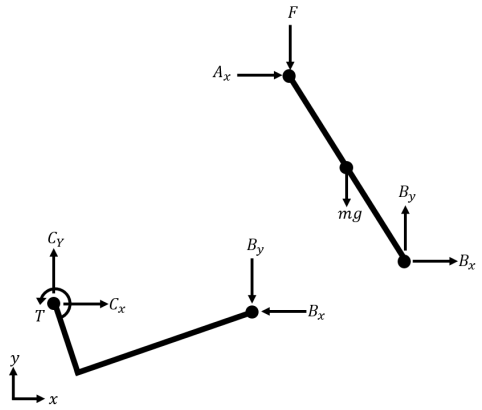

Figure 5.4: Free body diagram

$$
\begin{aligned}
A_x + B_x &= 0 \\
B_y - F - mg &= 0 \\
-mg\frac{b}{2}\sin(\alpha+\phi) + B_y b\sin(\alpha+\phi) + B_x b\cos(\alpha+\phi) &= 0 \\
B_x\cos(\alpha+\phi) &= mg\frac{1}{2}\sin(\alpha+\phi) - B_y\sin(\alpha+\phi) \\
B_x &= \sin(\alpha+\phi)/\cos(\alpha+\phi)(\frac{1}{2}mg - B_y) \\
&= \tan(\alpha+\phi)(\frac{1}{2}mg - F - mg) \\
C_x - B_x &= 0 \\
C_y - B_y &= 0 \\
T - B_y(a + e\tan\phi)\cos\phi - B_x(\frac{e}{\cos\phi} - d\tan\phi) &= 0 \\
T = (F+mg)(a+e\tan\phi)\cos\phi + \tan(\alpha+\phi)(-\frac{1}{2}mg - F)(\frac{e}{\cos\phi} - d\tan\phi) & \\
\text{where } A &\coloneqq (a+e\tan\phi)\cos\phi \\
B &\coloneqq \tan(\alpha+\phi)(\frac{e}{\cos\phi} - d\tan\phi) \\
T - mgA + B\frac{1}{2}mg &= F(A-B)
\end{aligned}
$$

resulting in

$$
\begin{aligned}
F &= \frac{T + mg(B/2 - A)}{A - B} \\
s(a,b,d,e,f,\phi) &= \sqrt{b^2 - [(a - e\tan\phi)\cos\phi - d]^2} - f - \frac{e}{\cos\phi} + [(a+e\tan\phi)\sin\phi]
\end{aligned}
$$

The full calculations to get α and s are in the MATLAB script.
Using the following dimensions from CAD

$$
\begin{aligned}
T &= 105mNm & e &= 6.5mm \\
d &= 20mm & b &= 72mm \\
f &= 55mm & a &= 40mm \\
m &= 20g
\end{aligned}
$$

we get (with LinearKinematicsTorque.m):

$$F(\phi = 40°, T) = 1.78N \qquad F(\phi = 40°, -T) = -2.11N$$
$$F(\phi = -40°, T) = 4.22N \qquad F(\phi = -40°, -T) = 4.64N$$
$$F(\phi = 0°, T) = 2.55N \qquad F(\phi = 0°, -T) = -2.9N$$

We see that the force needed to produce the required torque is greatest when $\phi = -40°$, because the effective lever arm becomes smallest. Correspondingly the force is smallest at $\phi = 40°$.

5.1.3 Internal Forces

The transmitting rod was also cut to determine the occurring internal force N:

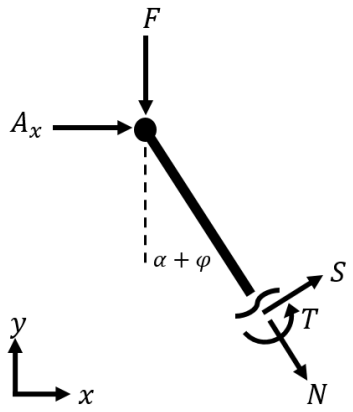

Figure 5.5: Free cut for internal forces

At $\phi = 40°, -T$ the internal force becomes largest with $N = 5.08N$. Assuming an aluminum rod and safety factor of 2 one gets a required cross section area of:

$$A = \frac{2F}{\sigma_{AL}} = 0.0508mm^2 = 0.225mm \cdot 0.225mm$$

One also calculated the required radius for the rod to avoid buckling:

$$\sigma_{crit} = \frac{\pi^2 E r^2}{(KL)^2}$$
$$r = \sqrt{\frac{\sigma_{crit}}{E}} \frac{KL}{\pi}$$
$$= \sqrt{\frac{FS}{\pi r^2 E}} \frac{KL}{\pi}$$
$$= \sqrt{\frac{FS}{\pi E}} \frac{KL}{\pi r}$$
$$r = \sqrt{\sqrt{\frac{FS}{\pi E}} \frac{KL}{\pi}}$$

with

$$E = E_{AL} = 73.1GPa \qquad F = F_{motor,max} = 10.7N$$
$$S = 2 \qquad K = 2$$
$$L = 55mm$$
$$\Rightarrow r = 0.6mm$$

The effect of impact loading on the rod did not have to be considered, because the motor would act as a mechanical fuse, where as soon as the motor's peak force is exceeded, the shaft is backdriven. Therefore the peak load that would act on the rod is the motor peak force. At the ends of the range of motion the joint ankle acts as a mechanical stop and bears all further loads.

5.1.4 Friction

Next the forces acting on the linear bearing inside the motor were determined, in order to find out whether they would cause to much friction and get stuck. The motor was modeled in Fig. 5.6 and the acting forces drawn.

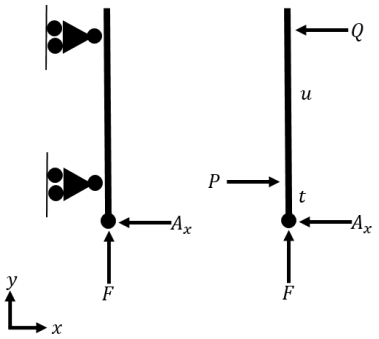

Figure 5.6: force on linear motor bearings for s=0, where the rod is maximally extended making a large lever arm.

Force balances give:

$$\begin{aligned} P - Q - A_x &= 0 \\ Qu - tA_x &= 0 \\ Q &= t/u \cdot A_x \\ P &= Q + A_x = A_x(1 + t/u) \end{aligned}$$

with

$$\begin{aligned} \phi &= -40^\circ & s &= 0 \\ u &= 41.8mm & t &= 64.7mm \\ T &= 105mNm & A_x &= -4.62N \\ \Rightarrow Q &= -7.15 \\ P &= -11.77N \end{aligned}$$

The resulting friction forces in Fig. 5.7 were also calculated.

$$\begin{aligned} F_f &= \mu \cdot |N| \\ F_Q &= \mu_{stat}|Q| \\ F_P &= \mu_{stat}|P| \\ \mu_{stat} &=\sim 0.8 \\ \text{with 2x safety } \mu_{stat} &=\sim 1.6 \\ \Rightarrow F_Q &= 11.44N \\ F_P &= 18.83N \end{aligned}$$

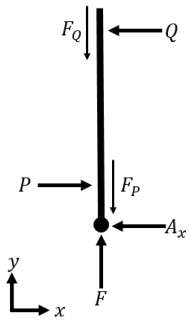

Figure 5.7: Friction in bearings

Because these combined are much higher than the motor's peak force, it would get stuck. This is why the design was altered so that the motor rod is aligned with the transmission rod and the transverse force A_x becomes zero, eliminating all friction induced by it.

5.2 Design Iterations

5.2.1 Linear Ankle Version 2

Next, a new version of the chosen linear motor design was made. In the meantime the design of the passive ankle had been largely finalized, so the model was updated accordingly (Fig. 5.8). The passive ankle now had a symmetrical foot, losing the taller ledge at the rear. The ankle joint had also been shifted from an off-center position to the middle of the sole.

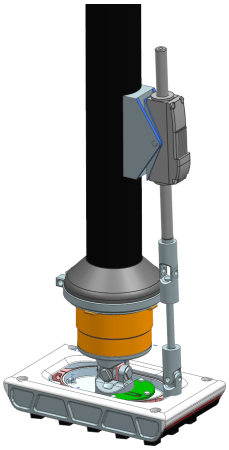

Figure 5.8: Linear ankle version 2

The new active ankle design adds a pivoting bracket, on which the motor is mounted. The pivot axis runs through the axis of the motor rod, which ensures that the forces between rod and motor are always along the axis of the bore, so that the rod does not get jammed in the bearings, due to transverse forces. Having gained an additional rotation axis in the transmission chain, one could be removed from the upper universal joint. Therefore the upper universal joint was replaced with a clevis joint.

One also investigated replacing the universal joint with a ball joint (Fig. 5.9). The smallest suitable one that was found uses a ball made of low friction bearing plastic. However it was too large and did not have sufficient roll range of motion. At full pitch extension (Fig. 5.9(b)), one can see how the ball joint would intersect with the force sensor.

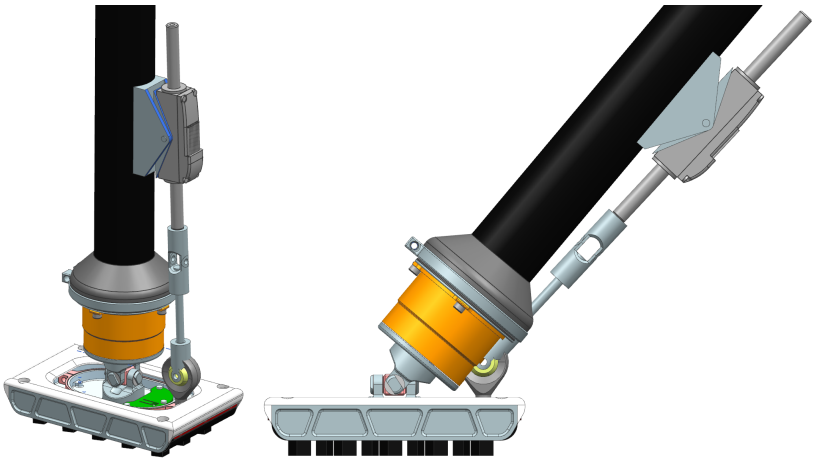

(a) Overview (b) Side view

Figure 5.9: Version 2 with ball joint

5.2.2 Linear Ankle Version 3

The third version (Fig. 5.10) brings a redesigned motor mount, where the motor is still on a swiveling bracket, but surrounded entirely by its counterpart mounted to the shank. The mount has openings on the top and bottom for the rod to move through and protects the motor from water and impacts. A compressible rubber sleeve would extend from the top of the mount around the rod to its top, where it would be fastened and sealed under a disk screwed onto the rod end. Correspondingly, a sleeve would cover the rod from the bottom of the mount over the joints and rod until the top of the foot.

Here the rod has been made as thin as possible just for illustration. If one were to make the rod out of steel, such a thin rod would still be sufficient to transfer the motors loads. However, such a thin rod would very quickly be bent out of shape or break upon any external impact.

In addition, plastic bearings were selected for the rod joints. The smallest possible ones were chosen, with a 1mm inner diameter by igus. In the clevis joint one bearing is used in the center, with a 1 mm axle going through. In the universal joint four are used, two per fork.

Lastly, a new damping system was created based on the existing rubber spring, but with an added mechanism that allows it to affect only one of both axes. Instead of covering the entire axle joint, the rubber spring only reaches up to the rotation axes. There, it is covered by a rigid ring with a flat upper surface, on which two pegs can roll. The pegs are connected to the shank so that they can transmit forces onto and compress the spring when the ankle rolls. They are also rounded at the ends, so that when pitching, they roll on the disk and barely compress the spring.

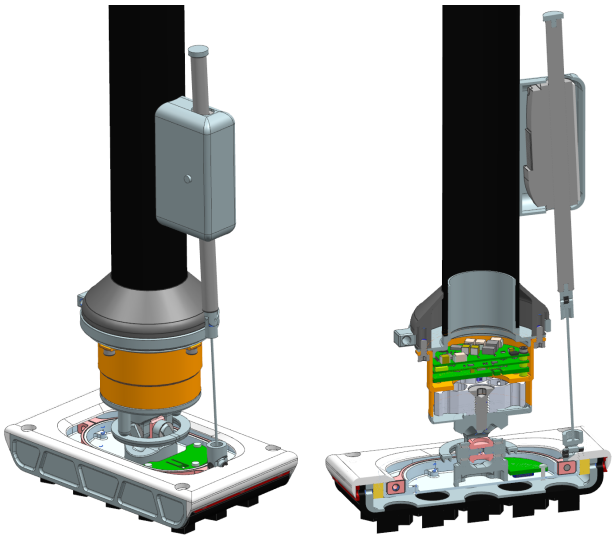

(a) Overview (b) Cross section

Figure 5.10: Linear ankle version 3

5.2.3 Linear Ankle Version 4

In the next major revision, the waterproofing system was rethought. The previous system of having both bellows at the joint ankle and over the transmission rod was deemed to complex, requiring seals at 4 points along the transmission mechanism. Furthermore having a cover over the universal joint ankles would additionally hinder them from bending. The two sleeves over the rod would also have to be compressed and stretched during every movement, weakening the effective power output.

Instead one opted to enlarge the bellow at the ankle to cover the entire motor and mechanism (Fig. 5.11), reaching from the foot up to a new top plate at the top of the shank. This way the bellow only has to be clamped at the top and bottom and seals everything at once. The top plate is screwed on to three curved parts that are clamped on to the carbon shank (Fig. 5.11(d)). On the upper side a flat ring compresses an O-Ring that seals the top plate.

No longer needing to seal the motor, the motor mount could be replaced by lightweight triangular supports. And the shank adapter made from aluminum was lengthened, so that the supports themselves could be attached. A small opening in the shank adapter allows the motor cables to pass through. The transmission mechanism was also simplified further, by aligning the lower universal joint with the joint ankle roll axis. By doing so, the clevis joint could be removed. In order to keep the same lever arm as in the motor calculations, the lower link of the universal joint had to be mounted in an overhanging manner to the internal sole. The top cover of the foot was modified accordingly, to prevent the bellow from being pinched when the internal sole would compress the foam and move relative to the outer hull of the foot.

The mounting position of the motor had to be finely selected, so that there would be no collisions during any point of the full range of motion. The position was selected so that when undeflected (Fig. 5.11(a)), the rod just barely does not touch the shank. At the same time, the rod must not stick out too much, since that would increase the required bellow size. When fully pitched in Fig. 5.11(c), the rod does not stick out much at the top, and the motor just barely does not touch the shank adapter. Similarly, the transmission mechanism is as close to the force sensor as

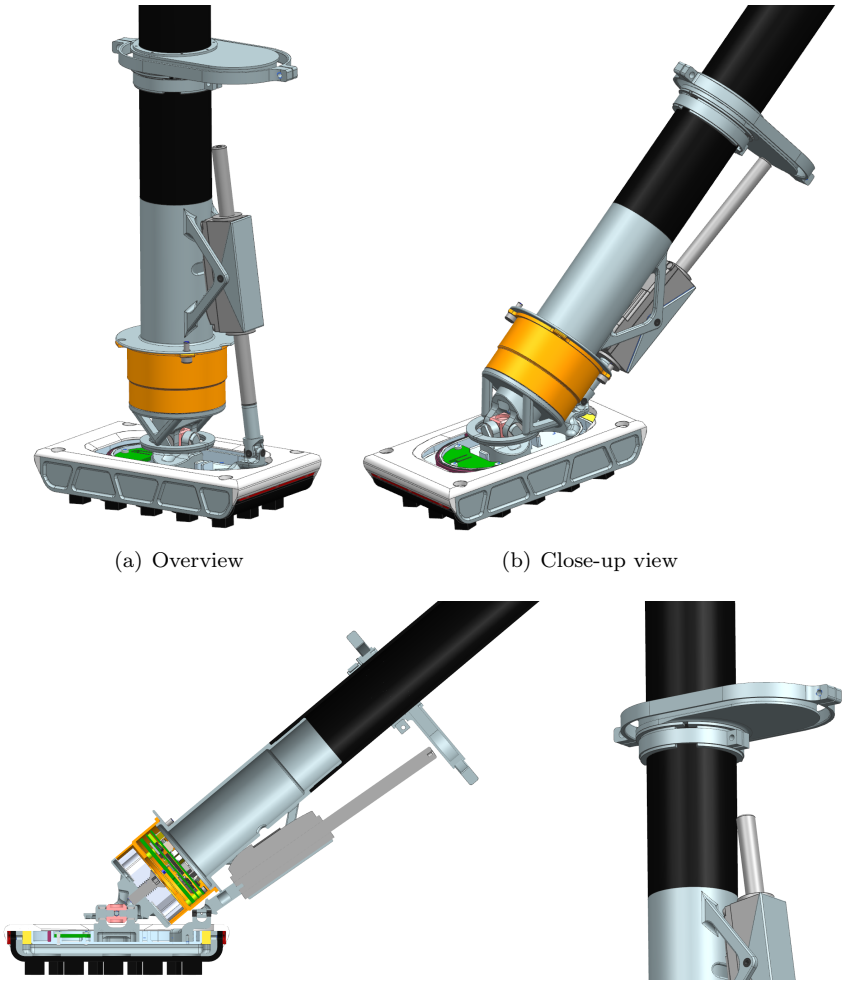

(a) Overview (b) Close-up view

(c) Cross section (d) Close-up view

Figure 5.11: Linear ankle version 4

possible. At the same time the motor was positioned low, in order to shorten the bellow, shank adapter and transmission rod lengths. Lastly, the damping levers were changed to triangular shapes, for more strength at high pitch angles.
This model was slightly modified for 3D-printing out of Nylon in a SLM-printer. All joints were realized with M2 screws as axles. The damping levers were also redesigned to be mounted on the upper fork, since their previous mounting position was not on a load bearing spot.
After sanding the joints and motor rod by hand, the prototype could be assembled without problems and worked as intended. The mechanism worked smoothly, enough to move under it's own weight. The damping system as also performed as designed, holding the foot without wobbling at the center position and buckling when rolling.
With the physical prototype, the force required to deflect the bellow could be measured on the model, since this would otherwise be very complicated and time-consuming to estimate. The previous bellow was mounted on the ankle and a cable-based scale attached to the motor rod. By pulling on the scale, the equivalent mass required to compress the bellow could be measured. However the measurements varied strongly from one another, ranging from 300 to 500g. In the case

of 500g, this would exceed the continuous force specification of the linear motor. Thereby the foot would not be able to hold its position indefinitely. For this reason, the next larger version of the linear motor was considered in the next version of the ankle.

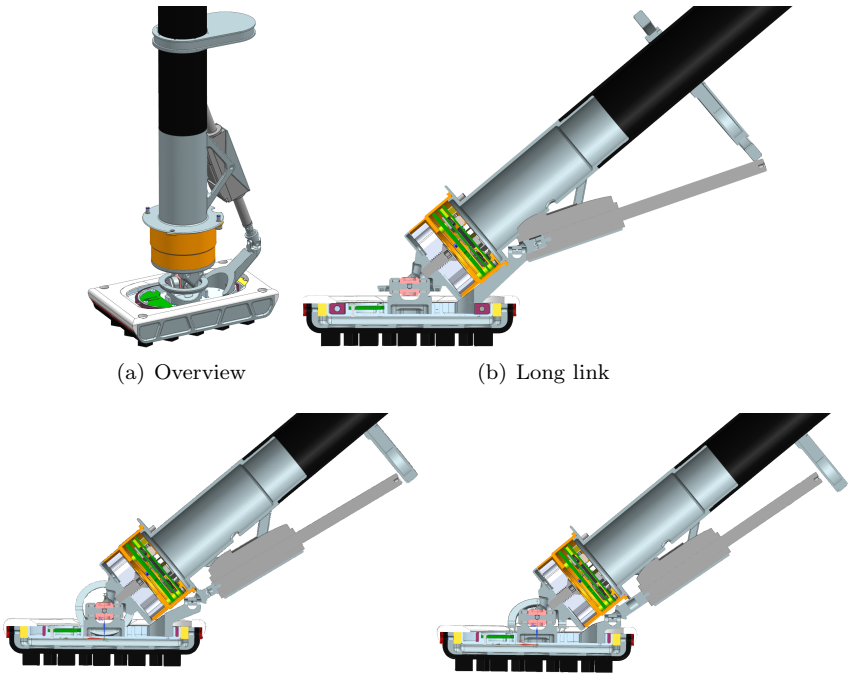

(a) Overview (b) Long link

(c) Medium link (d) Short link

Figure 5.12: Different lower link positions

Multiple variants of the lower universal joint link were explored in Fig. 5.12, with different joint positions and attachments to the internal sole. A longer, more stable link was tried in Fig. 5.12(a) with an added clevis joint for an out of axis universal joint. However this design did not provide more space for the bellow as hoped due to the force sensor and would have required the motor to be mounted higher up to avoid collisions during motion. Fig. 5.12(c) shows a slightly lower position, however again not resulting in any clear benefits. As a result the existing joint position was kept, with a reinforced lower joint link in Figure 5.12(d).

5.2.4 Linear Ankle Version 5

As stated previously, the larger version of the motor might be needed. So the ankle was redesigned to be able to house both versions of the motor (Fig. 5.13). This could be done relatively easily, thanks to the high flexibility of the chosen linear ankle concept. To this end, the triangular motor mount was decoupled from the shank adapter and screwed on instead. Rounded custom nuts would provide hold for the screws passing through the mount and shank adapter wall.
A corresponding motor bracket and mount were made for the larger motor (Fig. 5.14) and the shank adapter's height was adjusted to be able to fit both motor mounts. As with the smaller motor, the position of the large motor's mount had to be carefully set through multiple iterations, so that collisions are avoided and the motor does not lash out.
At the same time, the ankle joint was positioned out of center, in order to remove the

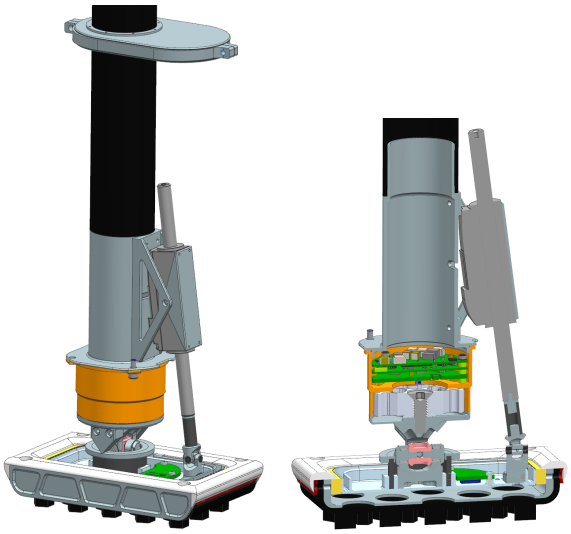

(a) Overview (b) Cross section

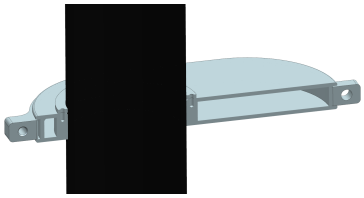

(c) Cross section of the top bellow plate

Figure 5.13: Small motor variant of ankle version 5

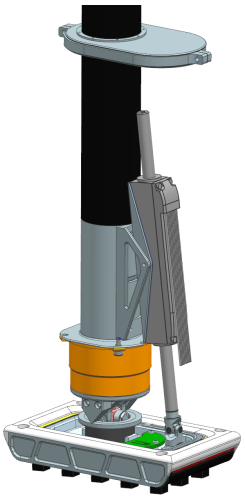

(a) Overview

Figure 5.14: Big motor variant of ankle version 5

need for an overhanging lower universal joint link. The ankle joint was positioned slightly less far out of center than in the first version of the passive ankle. This positioning also stops the bellow from being bent under the lower universal joint link.

The small motor's rod was also replaced by a glued short carbon fiber tube, to save a little bit of weight. And the top bellow mounting plate was simplified by gluing it to the carbon shank instead of clamping it (Fig. 5.13(c)). This plate could then be glued at the appropriate height for either of the motors. The bellow itself was also selected from hasler.ch, with a size large enough to fit the large motor ankle. The clamping ring on the sole was adjusted with the circumference of the bellow, as well as the top bellow mount. The largest diameter of the assembly is at the height of the shank adapter's flange. In CAD, a sketch with the selected bellow's diameter was placed at this height, in order to check if it would fit. Because it was tight, the flange was squared off here to make more room for the bellow. Furthermore, the top of the foot was adjusted to accommodate for the larger bellow.

5.2.5 Final Version

For the final version of the ankle, of which one unit would be produced, many fine details were finalized for manufacturing Fig. 5.15. For one, the top bellow mount was hollowed out and given ribs to reduce weight. Since this part would be glued, this would seal the gap with the carbon shank, which is why the O-Ring and matching clamp could be removed. One decided to 3D-print this part, because it would not need to carry any major loads. The carbon motor rod was replaced by elongating the upper universal joint link, combining three parts into one. Thereby making a simpler and not much heavier solution.
Apart from that, all fittings and tolerances were adjusted wherever multiple parts intersected. At the universal joint link Fig. 5.16(b), the joint would be held together by pins, press fit into the intermediate cube. The sleeve bearings themselves would also be pressed into the joint links, according to their manufacturer's specifications. At the motor joint (Fig. 5.16(c)), larger flanged bearings were picked instead, to offer greater axial support. These are mounted in the same manner. Pins with disk ends hold the joint together here.

5.3 Strength Calculations

5.3.1 Bearing Strength

The surface pressure on the bearing in the clevis joint was calculated, to see if it is not too high. D and L are the inner diameter and length of the igus iglidur M250 bearing. The considered surface is the projected part of the pin that is inside the bearing.

$$\begin{aligned}\sigma &= \frac{F}{DL} = \frac{10.7N}{1mm \cdot 2mm} \\ &= 5.35MPa < \sigma_{max,allowed} = 20MPa\end{aligned}$$

The resulting pressure shows plenty of safety, about 4x. Since the universal joint uses two bearings instead of one to bear the same load, it automatically will also be able to withstand the load with a higher safety factor.

5.3.2 Pin Strength

Then the shear forces in the pin were checked:

$$\begin{aligned}V &= \frac{F_V}{2A_{pin}} = \frac{F_V}{2\pi r^2} = \frac{10.7N}{2\pi(1mm)^2} \\ &= 1.71MPa < \sigma_{shear,AL} = 170MPa\end{aligned} \tag{5.1}$$

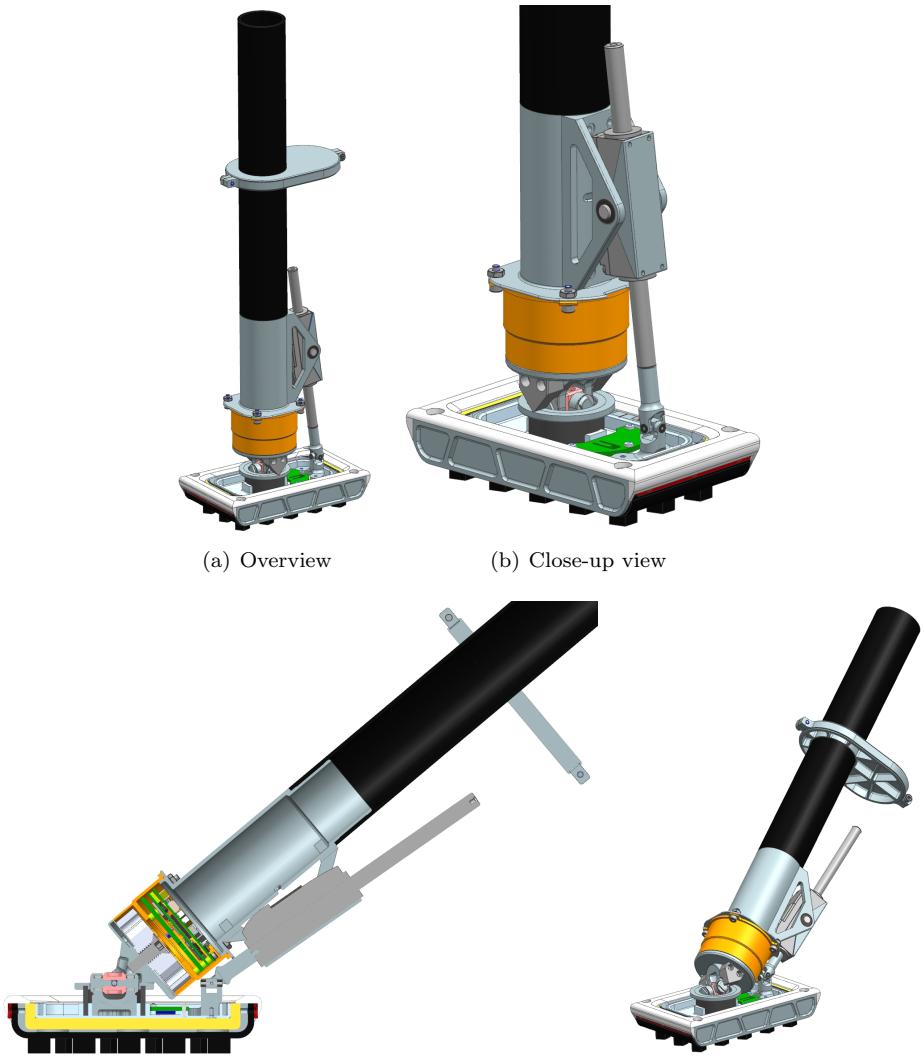

(a) Overview

(b) Close-up view

(c) Cross section at maximum pitch angle

(d) View showing the ankle at maximum pitch and roll deflections.

Figure 5.15: Final Version using the small motor

And the bending moment inside the pin:

$$M = a\frac{F}{2} = 1mm \cdot 0.5 \cdot 10.7N = 5.4mNm$$

$$\sigma_{max} = \frac{My}{I} = \frac{Mr}{\frac{1}{4}\pi r^4} = \frac{M4}{\pi r^3}$$

$$= 6.8MPa < \sigma_{yield,AL} = 414MPa$$

In both cases we get very large safety factors.

5.3.3 Universal Joint Cube Strength

The normal and shear stresses inside the universal joint cube were verified, where the pin presses on the inside of the cube. At this point the larger motor was also

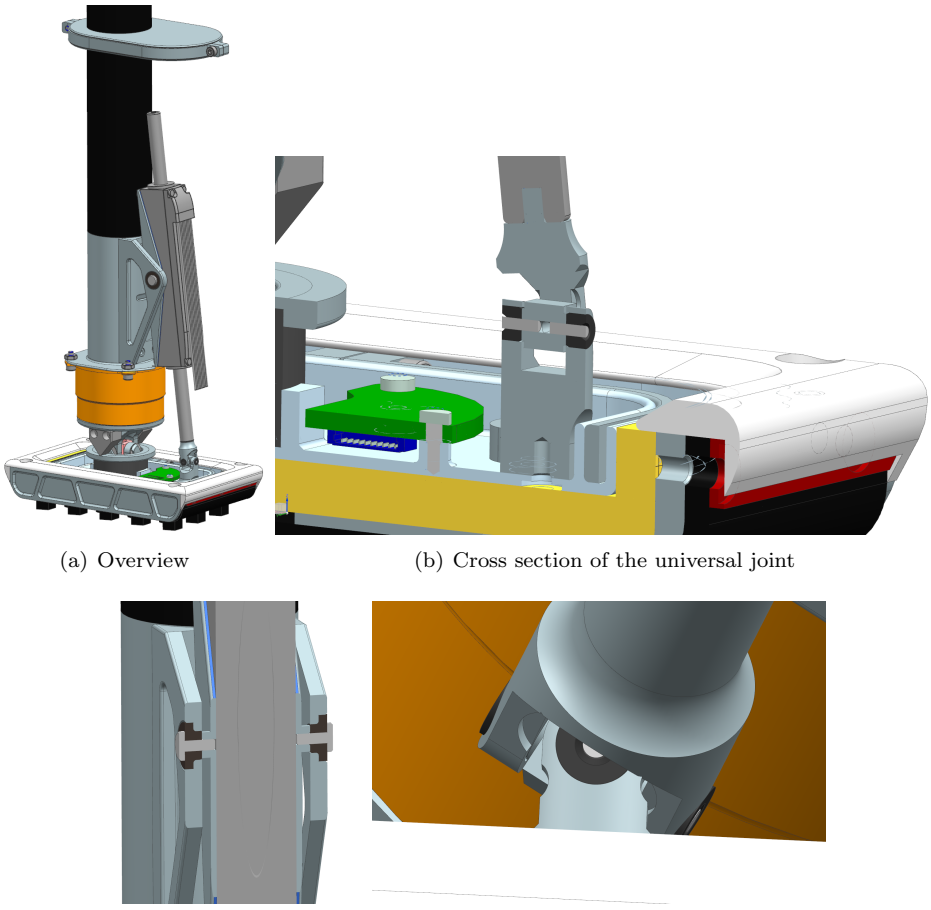

(a) Overview

(b) Cross section of the universal joint

(c) Cross section of the motor joint

(d) Cutouts to avoid collisions at maximum deflection of the joint

Figure 5.16: Final Version using the big motor

considered, which is why F is higher than previously.

$$\begin{aligned}\sigma &= \frac{F/2}{DL} = \frac{18.4N/2}{1mm \cdot 1mm} \\ &= 9.2MPa < \sigma_{yield,AL} = 414MPa \\ V &= \frac{F/4}{Lh} = \frac{18.4N/4}{1mm \cdot 1.5mm} \\ &= 3MPa < \sigma_{shear,AL} = 172MPa\end{aligned}$$

5.3.4 Universal Joint Fork Strength

Calculated at the smallest cross section of the fork on the height of the pin under tension.

$$\begin{aligned}\sigma &= \frac{F/2}{A} = \frac{10.7N}{2 \cdot 0.5mm \cdot 1.5mm} \\ &= 7.13MPa < \sigma_{yield,AL} = 414MPa \\ \epsilon &= \frac{\sigma}{E} = 0.0097\%\end{aligned}$$

As for the shear forces caused by the intermediate cube being pushed in axial direction of the pin, at maximum pitch deflection of 50°, we get

$$F_V = \frac{1}{2} F \cos 50° = 6.88N$$

Because we get a lower shear force than $F_V = 10.7N$ in the case of the pin shear in (5.1) and the affected surface is larger than the pin cross section in that case, we can already conclude that the shear strength will be sufficient.

5.3.5 Damping Lever Strength

Here the forces in the damping lever were calculated. First we get the moment needed to compress the spring from the measurements with the scale:

$$\begin{aligned} F_{spring,test} &=\sim 11.8N \\ M_{spring,test} &= F_{spring,test} \cdot a = 11.8N \cdot 25.5mm = 300mNm \end{aligned}$$

Then we determine the resulting force on the lever and the ensuing shear and bending stresses in the two screws:

$$\begin{aligned} F &= \frac{M_{spring,test}}{a_{damp.lever}} = \frac{300mNm}{12.96mm} = 23.2N \\ \sigma_V &= \frac{F}{2A_{screw}} = \frac{F}{2\pi(D/2)^2} = \frac{23.17N}{2\pi(1.8mm/2)^2} = 4.55MPa \\ &= 4.55MPa < \sigma_{shear,AL} = 172MPa \\ M &= a_{lever-screw} \cdot F/2 = 2.47mm \cdot 23.2N/2 = 28.62mNm \\ \sigma_B &= \frac{My}{I} = \frac{Mr}{\frac{1}{4}\pi r^4} = \frac{M4}{\pi r^3} \\ &= 2.33MPa < \sigma_{yield,AL} = 414MPa \end{aligned}$$

Next the pressure along the line where damping lever and the ring meet was determined. First the peak occuring stress along the line is calculated, so that then the safety factor can be obtained while accounting for a lower stress at other points along the line [19].

$$\begin{aligned} \sigma_{max} &= \sqrt{\frac{F(\frac{1}{r_1} + \frac{1}{r_2})}{\pi(1-\nu^2)(\frac{1}{E_1} + \frac{1}{E_2})L}} = \sqrt{\frac{F\frac{1}{r_1}}{\pi(1-\nu^2)\frac{2}{E}L}} = \sqrt{\frac{FE}{\pi(1-\nu^2)r_1 2L}} \\ &= \sqrt{\frac{23.17N \cdot 73.1GPa}{\pi(1-0.35^2)0.5mm \cdot 2 \cdot 5.4mm}} = 337.3MPa \\ S &= \frac{\sigma_{yield,AL}}{\sigma_{max} \cdot 0.608} = 2 \end{aligned}$$

5.3.6 Rubber Spring Holder

Next we check the bending and shear stress inside the ring on top of the spring, the rubber spring holder. We approximate the ring as seen from the side by a single straight bar. For the yield strength we use the value of DuPont Delrin 100 BK602

Acetal Resin as an estimate.

$$\begin{aligned} M &= \frac{F}{2}r \\ I &= \frac{1}{12}bh^3 \\ \sigma &= \frac{My}{I} = \frac{Mh/2}{I} = \frac{Mh12}{2bh^3} = \frac{6M}{bh^2} \\ &= 15.36MPa < \sigma_{yield,delrin} = 72MPa \\ V &= \frac{F}{2} \\ \sigma_V &= \frac{V}{A} = \frac{V}{bh} = \frac{F}{2bh} \\ &= 0.4MPa \end{aligned}$$

The shear strength value was not provided, however the resulting stress is reasonably low enough.

5.3.7 Motor Triangle Strength

Next we check the bending stress inside the arm of the motor triangle, in which the motor is mounted on a pivoting bracket. We assume that the triangle is perfectly symmetrical and get:

$$\begin{aligned} M &= \frac{F}{4}a \\ I &= \frac{1}{12}bh^3 \\ \sigma &= \frac{My}{I} = \frac{Fay12}{4bh^3} = \frac{3Fay}{bh^3} = \frac{318.4N \cdot 13.6mm \cdot 2mm}{1mm \cdot (4mm)^3} \\ &= 23.5MPa < \sigma_{yield,AL} = 414MPa \end{aligned}$$

5.3.8 Shank Adapter Strength

In order to gauge whether making holes inside the shank adapter would be an issue, the safety factors of the normal and bending stress were calculated:

$$\begin{aligned} \sigma_N &= \frac{F}{A} = \frac{F}{\pi(R^2 - r^2)} = \frac{300N}{\pi((15mm)^2 - (13.5mm)^2)} = 2.23MPa \\ S_N &= \frac{\sigma_{yield,AL}}{\sigma_N} = 185.7 \\ \sigma_y &= \frac{My}{I} = \frac{FLD/2}{I} = \frac{FLD4}{2\pi(R^4 - r^4)} = \frac{2FLD}{2\pi(R^4 - r^4)} \\ &= \frac{2 \cdot 300N \cdot 60mm \cdot 30mm}{2\pi((15mm)^4 - (13.5mm)^4)} = 2.23MPa \\ S_y &= \frac{\sigma_{yield,AL}}{\sigma_y} = 21 \end{aligned}$$

There is enough headroom to accommodate even large stress rises caused by holes.

Chapter 6

Alternative Designs

After completing the linear ankle design, some alternative versions were explored. A different version of the linear ankle and a new design, the bowden ankle.

6.1 Linear Ankle

For added protection a modified foot with raised corners and a motor cage were designed (Fig. 6.1). The new foot prevents more objects from hitting the universal joint and the cage protects the motor more. When fully deflected, they together shield almost the entire bar mechanism.

The top bellow holder already ensures that when the foot hits against a flat surface, the motor does not get hit, no matter the angle. The motor cage however adds additional protection from smaller protruding objects. Whether this is necessary could be seen later when testing ANYmal in the real world.

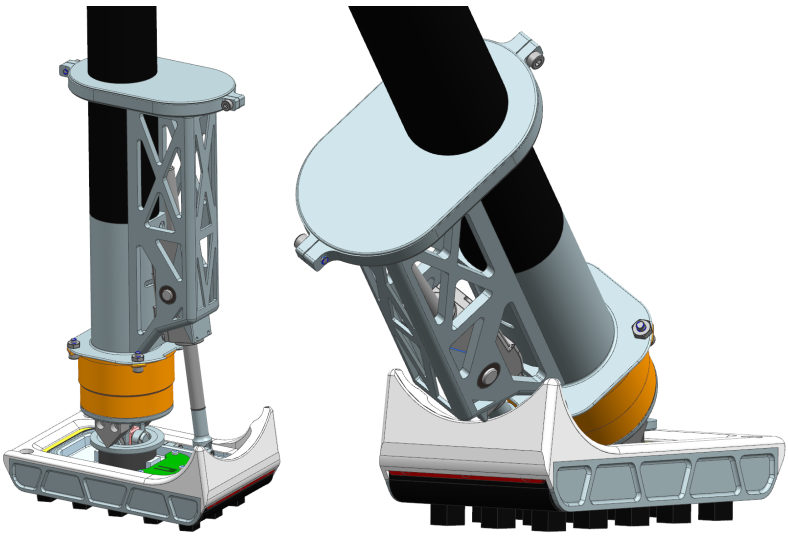

(a) Overview (b) At maximum deflection

Figure 6.1: Additional motor and rod protection

6.2 Bowden Ankle

One also looked at using a bowden cable instead of the bar mechanism. Using this transmission, a new design would be possible, where the motor could be placed near to the knee joint to decrease the inertia w.r.t. the knee. This would also remove the necessity that the bellow cover the motor rod. Instead it could only cover the ankle joint as in the passive ankle.
A new design with the bowden cable was created and modeled in CAD Fig. (6.2), where the motor is placed inside the carbon shank and centered heightwise with the knee joint. This means that the motor rod will protrude when moved, but having the motor as high up as possible gives the bowden cable a longer distance along which to bend, reducing the friction inside. The protruding rod could be covered by a simple cylindrical cap, that also holds the motor mount in place by attaching to the knee joint clamps.

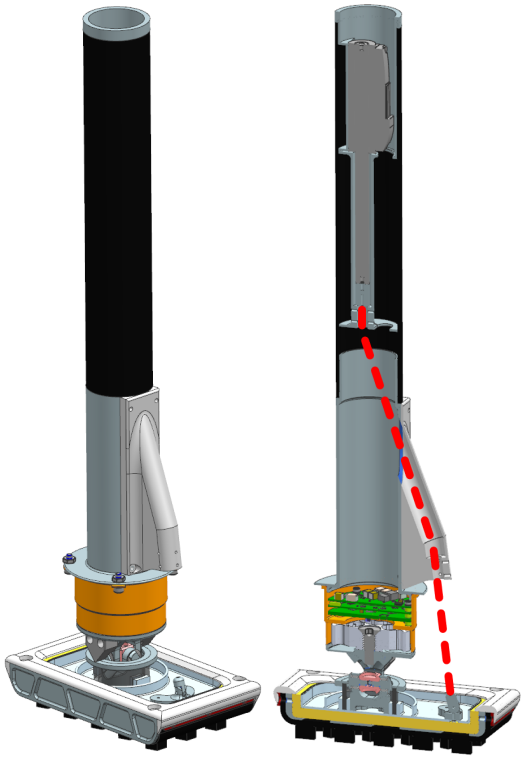

(a) Overview (b) Cross section

Figure 6.2: Bowden ankle

The motor itself is mounted in a tube that slides into the top of the carbon tube. A smaller tube extends down around the motor rod until a section where the bowden cable can be mounted and held in place by tightening screws. The disk at the bottom of the motor tube helps the narrow tube section stay in place by touching the insides of the carbon tube. Additionally, cutouts om the motor tube allow cables to pass through from below.
Further down the bowden cable passes through an elongated shank adapter, to which a new mount is attached that guides the cable towards the heel. This mount is shaped as long as possible, in order to bend the cable as gently as possible towards the motor to keep down the friction. The point and angle at which the bowden cable exits the shank mount were set equal to where the rod exits the motor in the linear

ankle. There tests had shown that the moment arm was sufficient.
At the internal sole the cable is mounted to a clevis joint. Tests with a 3D printed prototype with a rigid attachment instead had proven unsuitable, because at the outermost pitch angles the cable would bend so much that further movement was blocked.

Chapter 7

Production

One unit of the linear active ankle was planned to be produced using various manufacturing methods for different parts. Non-load-bearing parts such as the top bellow mount would be 3D-printed, while most load-bearing parts would be machined from aluminum by a shop. For these parts technical drawings were made, detailing the size of the initial block of metal, all holes, threads and tolerances. The type of aluminum used is the same as for the passive ankle. Some of the less critical parts would be machined out of POM, such as the rubber spring disk, where it would also lead to lower friction where touching the aluminum damping levers.
The carbon rod was cut to length and all necessary screws, bearings and other parts ordered. Because the machine shop where the aluminum and POM parts were to be machined already had an unusually long backlog of pending orders, they would not have been fast enough to machine all parts in time. Which is why only the most critical parts were sent into production, such as the ankle and universal joint. The remaining parts were 3D-printed and then assembled as seen in Figure 7.1(a). On the other hand, the bowden ankle was entirely 3D-printed in prototype form.

(a) Linear ankle with mounted bellow. For testing purposes with a shorter shank.

(b) Bowden ankle

Figure 7.1: Manufactured and assembled ankles

Chapter 8

Low Level Control

8.1 Setup

In order to test, run and write programs to control the motor, the etherCAT version of the Faulhaber MC 5004P Motion Controller was used. For testing purposes, the smallest controller that was compatible with the motor and etherCAT was chosen. Later on one could find or make a smaller solution to fit inside the shank. The motor was connected to the motion controller according to the connection diagram in appendix A. Then the controller was connected to a KORAD KD6005P programmable DC power supply (0-60V, 0-5A) set to a constant 48V. For this connection cables with Molex connectors were soldered, so that one can easily switch between the power supply and ANYmal's power. For initial setup the controller has to be configured with Faulhaber Motion Manager, for which the controller was connected via micro USB on Windows. Over this connection programs in BASIC were also written and run, as described later.

8.2 Control over Motion Manager

Motion manager allows simple manual control through a GUI for testing and troubleshooting, but to test proper operation the following programs were written. The motion controller can be entirely controlled by changing values of its object dictionary, which contains status information about the drive and control settings, such as target position and gain values. Status- and controlword can also be addressed this way. So the most important commands are GETOBJ and SETOBJ, which read and set values of the dictionary respectively.

8.2.1 Tuning

The controller uses cascaded control with an innermost loop for current/torque, then velocity and position. It was tuned using the tuning tool in Motion Manager, where the gain values can be changed interactively while continuously recording step responses and seeing how they change. Fig. 8.1 shows the step response of the linear active ankle and Fig. 8.2 the one of the bowden ankle before and after tuning.

8.2.2 Homing

Because the integrated Hall sensors are only relative, the range limits need to be redetermined at each powering on. Otherwise one could command a position that

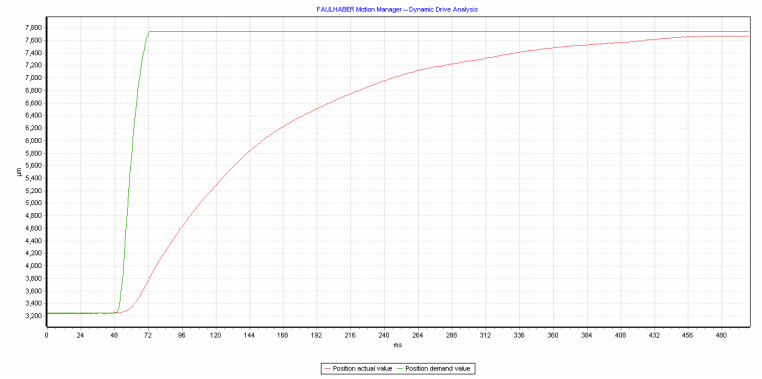

(a) Before

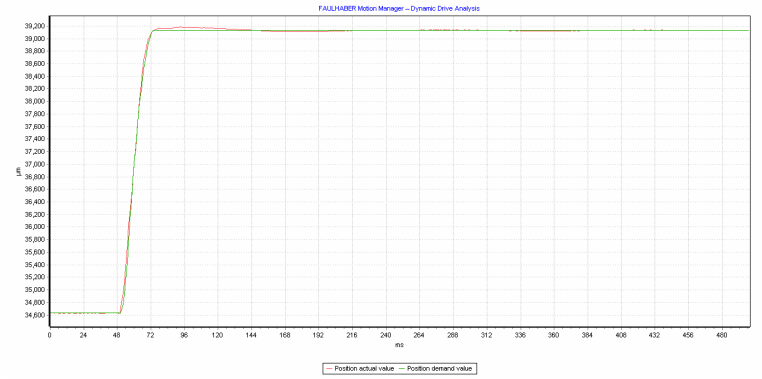

(b) After

Figure 8.1: Linear ankle tuning

would eject the rod from the motor. At the same time one then knows the zero position of the motor. This could even be done manually in the GUI for initial testing, but soon an automated script was needed.

The program first enables the motor and then sets it into profile position mode. After which the previous maximum positive and negative torque limits and velocity are read and stored for restoration later. Then all of these values are lowered and the motor moves in one direction until its velocity is close to zero when it reaches the block. This position is saved and the same is repeated in the opposite direction. In the end the position range limits are set to these values with a small added margin to allow some overshoot. And the torque and velocity limits are reset too.

8.2.3 Back and Forth Movement

In this script the motor simply moves from end to end as quickly as possible. The time between which the commands to move to the next end are issued can be set, so that it makes a movement every chosen amount of seconds.

In the beginning it starts the motor up again and goes into profile position mode. After reading the position limits it cyclically moves from limit to limit while waiting the set amount of time in between. The move() function first sets the object for the goal position and then sets the object that tells it to move to the goal position. In profile position mode, the controller then computes a motion profile to get there and executes it.

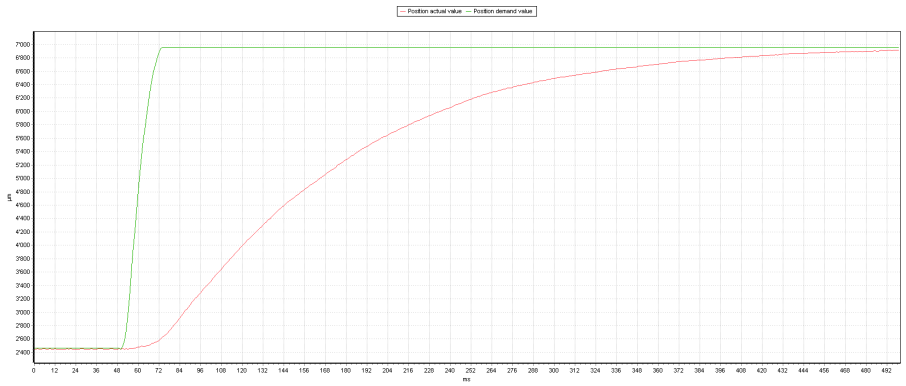

(a) Before

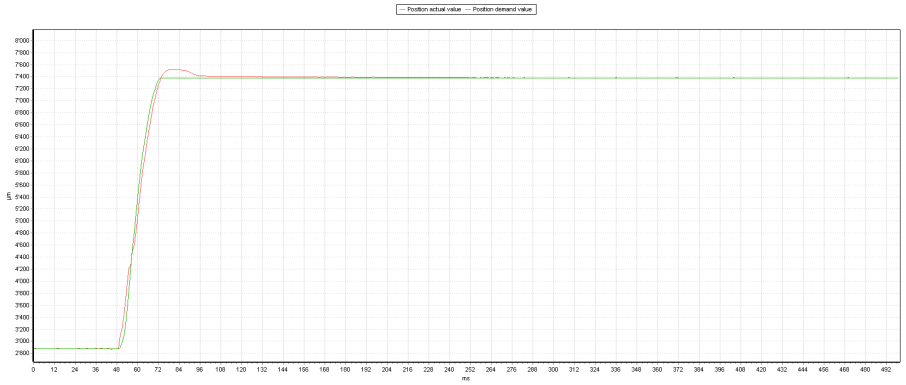

(b) After

Figure 8.2: Bowden ankle tuning

8.2.4 Compliant Control

One was also able to achieve compliant behaviour of the ankle, by reducing the force limits of the motor. If one then simply sets the ankle to a certain position, it will try to hold that same position. Through the reduced force, the cascaded controller is still in full effect without needing to change any of its gains. Then one can easily deflect the ankle without much resistance and it simply moves back upon release. By setting the force limits to the continuous force of the motor, the ankle can be deflected from its setpoint multiple times or indefinitely without overheating. It behaves similarly to the passive ankle, with the advantage that the neutral position can be arbitrarily selected and changed. This was also tested by hand by mimicking the walking motion of ANYmal. The ankle position can be set to hold the angle at which the foot normally lands. While in ground contact, the ankle can then be moved by backdriving the motor and upon lift off the ankle returns back to the desired position, ready for landing.

8.2.5 Dual Control

Dual control works like the back and forth script, except that in the stance phase the force limits are set to zero, so that the ankle does not resist at all during the passive phase. Later, when the ankle is integrated with the other sensors on the foot and ANYmal, this should be triggered when contact with the ground is sensed. One possible controller at that point would be to combine all three of the above

features. After lift off, the force limits would be set to the maximum, so that the target angle is reached as quickly as possible. For the remaining flight phase, the limits can be set to the continuous force, so that the position is still held, but upon any external disturbance and on impact with uneven ground it would act compliantly. After waiting a short time after touchdown to ensure full ground contact in the event of bounceback or similar, one could set the forces to zero for the passive stance phase.

8.3 Control over EtherCAT

In order to prepare the ankle for use on ANYmal, the ankle was made controllable over EtherCAT on ROS.

8.3.1 Connection

A new package called ankle-ethercat was created for the ankle. A new EtherCAT slave class called AnkleEtherCatSlave was created for the ankle, which is a class derived from the EtherCatSlaveBase class. This class works together with the EthercatBusBase class, that manages the bus on which there can be multiple slaves. AnkleEtherCatSlave implements the virtual functions defined in the parent class for the ankle. These cover reading and writing TxPDOs and RxPDOs over which continuous data can be read or sent. They were configured to handle one type of RxPDO and TxPDO each. They also handle startup and shutdown of the slave. SDOs for singular data readings or writings can be sent and read via the EthercatBusBase.
In order to test this on a laptop, a main.cpp program was written which first creates an EthercatBusBase object for the connected Ethernet port. Then an AnkleEtherCatSlave object is created for the ankle and added to the EthercatBus. The bus is then set into operational state after which communication can start.

8.3.2 Control

The previous control scripts in BASIC were rewritten in C++ to test control over EtherCAT. These could be implemented using only SDOs, because sending and writing SDOs is equivalent to SETOBJ and GETOBJ. The parts of the libraries MotionMacros and MotionParameters that had been used were ported and various functions rewritten into the main file. The first of which is the function Enable() which puts the motor into operating mode. Then there is a timer function IsTimeElapsed() and functions for moving to relative and absolute positions MoveRel() and MoveAbs. Lastly there are the control functions from the last section, Homing(), BackNForth(), and CompliantHold(). All of which were run successfully on the ankle by calling them in the main file.

Chapter 9

Testing

9.1 Range of Motion

The pitch range of motion was verified optically in Kinovea for both ankles (Fig. 9.1) and limits. For the linear ankle we get approximately ±50°, exceeding the minimum requirement of ±40° by a total of 22°.

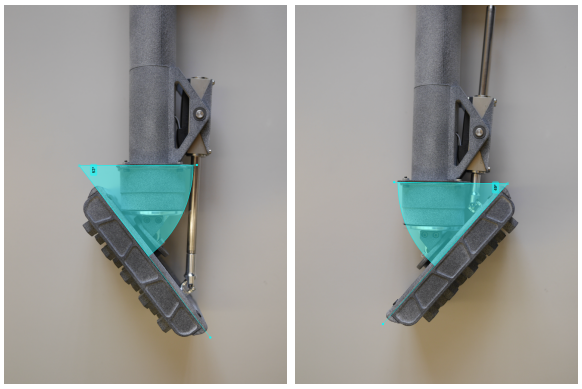

(a) 53° (b) 49°

Figure 9.1: Linear ankle pitch range of motion

In the bowden ankle we again get 50° on one side and ca. 40° on the other. This could be evened out by readjusting the cable length to about ±45° instead, again exceeding the demanded specifications. In reality both ankles have slightly larger ROMs than measured, because they are photographed in a slacking position. A few extra degrees can be gained by pushing against the rubber spring which comes into contact at that point and by fully tensioning the bowden cable.

9.2 Speed

In order to test the pitch repositioning requirement of 0.3s, the ankle was moved from end to end in a step response. Target and actual position were graphed in Motion Manager. This is shown in Fig. 9.3 for the linear ankle with the bellow mounted moving in both directions. The resulting step times of 91 and 110ms make for a safety factor of roughly 3, far exceeding the requirement. Because this is for the entire range of about 50°, the safety factor is actually even higher because the requirement was set for the minimum demanded ROM of ±40°.

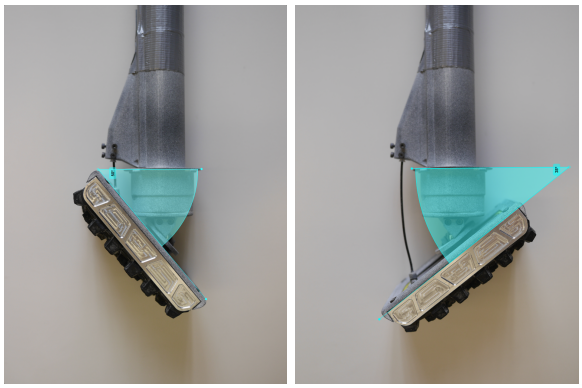

(a) 50° (b) 38°

Figure 9.2: Bowden ankle pitch range of motion

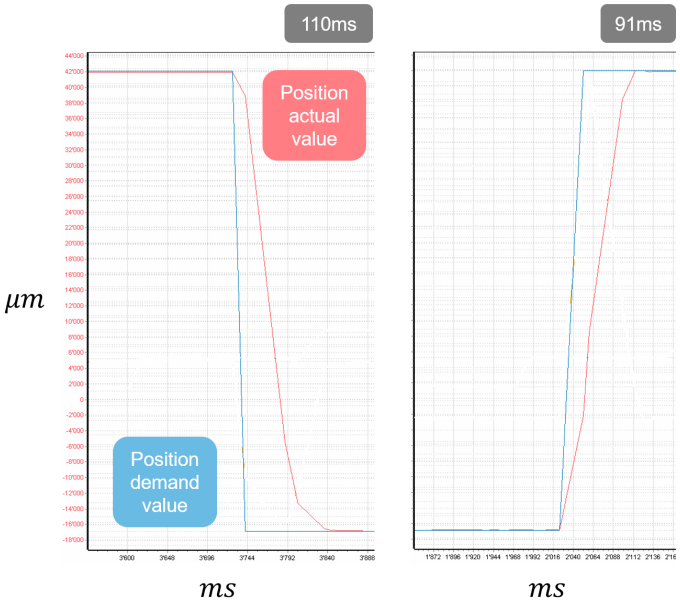

Figure 9.3: Upward movement of the rod in 110ms, downward in 91ms, for the linear active ankle with bellow and full range. Unfortunately Motion Manager does not allow resizing the axes, which is why the graphs is not optimized for this size.

The same test results are shown for the bowden ankle with mounted bellow in Fig. 9.7. Despite the added bowden cable friction, the step times are similar and even lower for the upward movement. Most likely due to the smaller bellow and thus smaller amount of material that has to be moved. Probably the motor has enough force headroom to overcome the added cable friction, which is why it still performs similarly quickly. If this is the case it most likely leads the motor to generate more heat.
The ankles were also operated in dual control mode and graphed (Fig. 9.5), to see their performance during typical operation. As expected, the step times are as sufficiently fast .
As for the positioning accuracy, it is easily sufficient for aligning the foot before touchdown and thus fulfills this requirement. Notably the linear motor is highly accurate with an accuracy of 140 µm. On top of that the transmissions add a

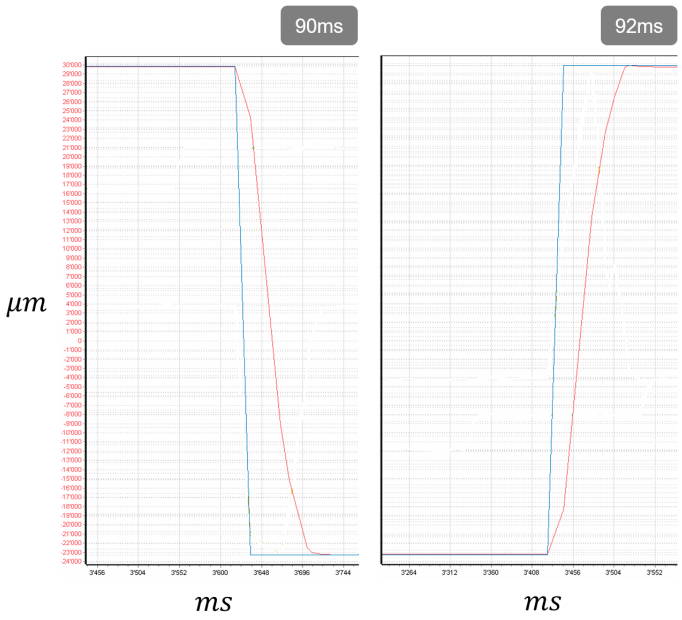

Figure 9.4: Upward movement of the rod in 90ms, downward in 91.9ms, for the bowden ankle with bellow, and full range.

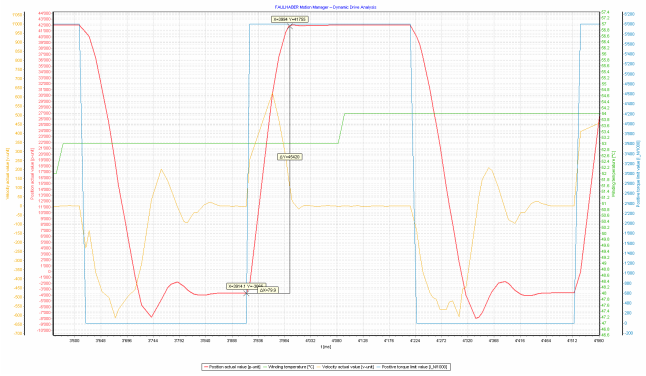

(a) Linear ankle: 79.9 ms

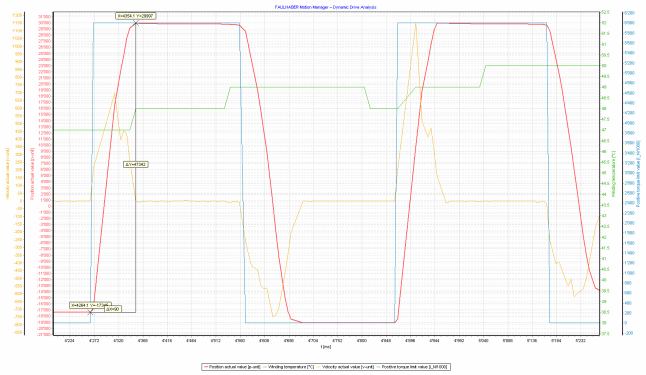

(b) Bowden ankle: 90 ms

Figure 9.5: Dual control operation

manageable amount of play.

9.3 Temperature

The temperature development in the motor over time was also tested, by running the DualControl script for shy of 2 minutes and deflecting the foot in the passive phase by hand. The stance and swing times were both set to 300ms and the movement covered the full range. In this case (Fig. 9.6(a)) the recorded temperature of the linear ankle rose quickly at an unsustainable rate. However it was observed by testing that when idling at one of the range ends, the temperature would keep rising, whereas at all other positions it would not. This could be due to the bellow being slightly too short at that position, which would mean that the motor would constantly have to push against it. It could also be that during homing the mechanism was elastically slightly deformed by the pushing motor, because of the flexible 3D-printed parts. This would again mean that it would keep pushing against the structure and build up heat.
So the target position at that end was slightly reduced and the test rerun. As hoped the temperature stayed much lower (Fig. 9.6(b)). In actual use when walking the temperature should not be an issue, because during most steps the ankle will only move a small portion of the full range tested here.

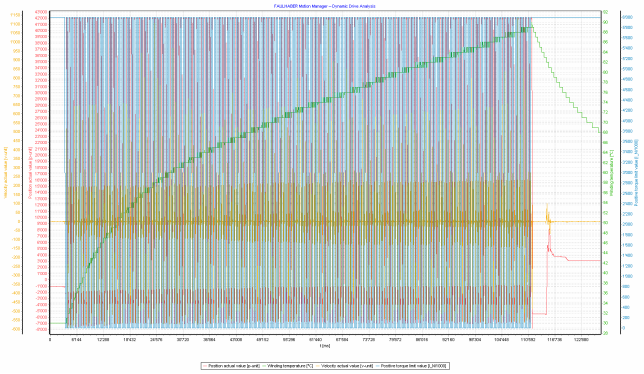

(a) Full range, 30-89°C

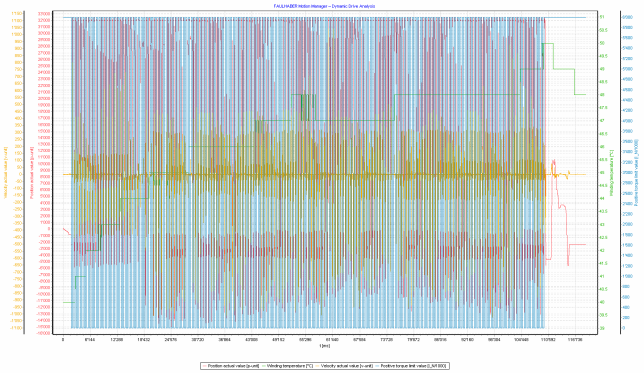

(b) Reduced range, 40-50°C

Figure 9.6: Temperature test of the linear ankle with bellow

The same test was performed on the bowden ankle in Fig. 9.7.
For the full range the temperature first rises rapidly and then transitions to a linear

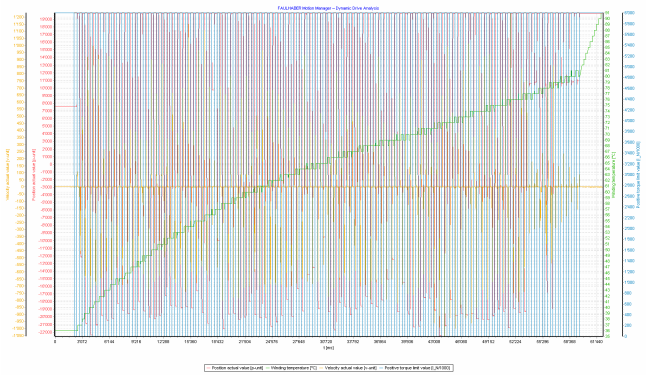

(a) Full range, 36-81°C

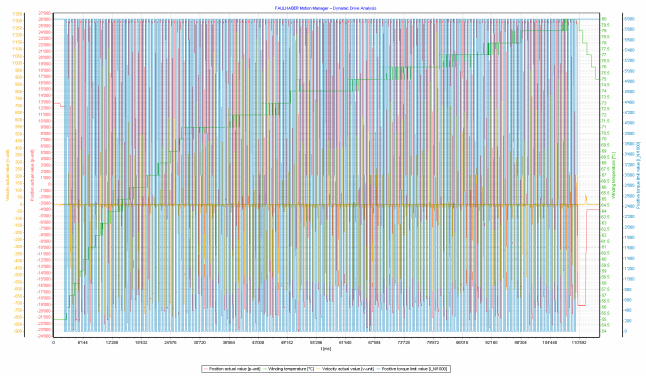

(b) Reduced range, 55-80°C

Figure 9.7: Temperature test of the bowden ankle with bellow

increase. For the slightly reduced range the temperature again rises steeply at the start, but then flattens out more towards the end. Overall the temperature difference from start to finish is lower with 25° opposed to 45°C.
The main issue is the bellow compression at large deflections, where the motor has to constantly push against it. The bellow used in the prototype is made from a rolled sheet which is wound into a tube by gluing overlapping edges. This overlapping area runs along the tube in a spiral and is a lot more stiff. So the bellows were mounted so that these areas get bent as little as possible. However in the bowden ankle the bellow is clamped in a circle, which means more of the stiffer area reaches into the compressed zone. In contrast in the linear ankle the clamp is rectangular, giving more space within which the stiff line can be placed.
Again, during real life operation the heat development will likely not be an issue, otherwise there is still room to optimize the bellow solution.
And if overheating still became problematic in the future, one could try to mount a sort of propeller on the top end of the motor rod. When actuated, the propeller would move up and down and create cooling airflow inside the shank.

9.4 Mass

Because the ankles did not have their final parts, their masses were roughly estimated from CAD, by measuring the assembly's volume. All parts were approximated as being made from aluminium, except the carbon shank from carbon. Some

parts not contained in the model were omitted such as the bellow. For the linear ankle one gets:

$$m_{AL} = 270.46g$$
$$m_C = 40.7g$$
$$m_{tot} = 374g$$

And for the bowden ankle with the full calculations:

$$m_{AL} = \rho_{AL} V_{AL} = 2.79g/cm^3 \cdot 110563.26mm^3 = 308.47g$$
$$m_C = \rho_C V_C = 1.55g/cm^3 \cdot 110563.26mm^3 = 35.5g$$
$$m_{tot} = m_{AL} + m_C + (m_{mot} = 63g) = 407g$$

The estimated mass of the linear ankle is lower, but it might be offset by the larger bellow, so in the end both variants have a comparable weight.

9.5 Testing on ANYmal

Lastly the bowden ankle was tested on ANYmal. For testing a controller case was designed to mount it on the knee in place of the knee pad. Fig. 9.8 shows how it screws on with a flange, and internally one of the PCBs is fixed by screws. Additionally it is held in place through the case's shape.

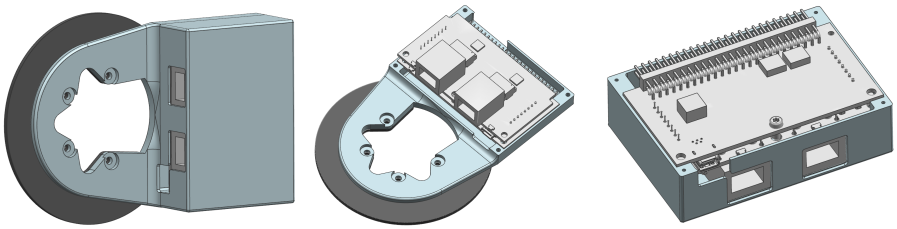

(a) Overview (b) Bottom (c) Top

Figure 9.8: Controller Case with ports for header pins, EtherCAT and micro USB

The encased controller was mounted and connected directly to the ankle (Fig. 9.9). Inside the thigh one of the power cables going between the ANYdrives of the knee and hip was replaced by one that had a junction with a Molex connector, to which the controller was connected for 48V power. The controller would also have the option to store programs and automatically run them when turned on, but it was controlled via USB instead. The ankle was able to support the robot weight with only the 3D-printed parts. Powering the ankle worked without problems and the homing and back and forth programs were successfully tested. It was also able to walk while the ankle held its position. ANYmal was even able to wave for the first time by running a high-five sequence to raise its paw and then moving it back and forth.

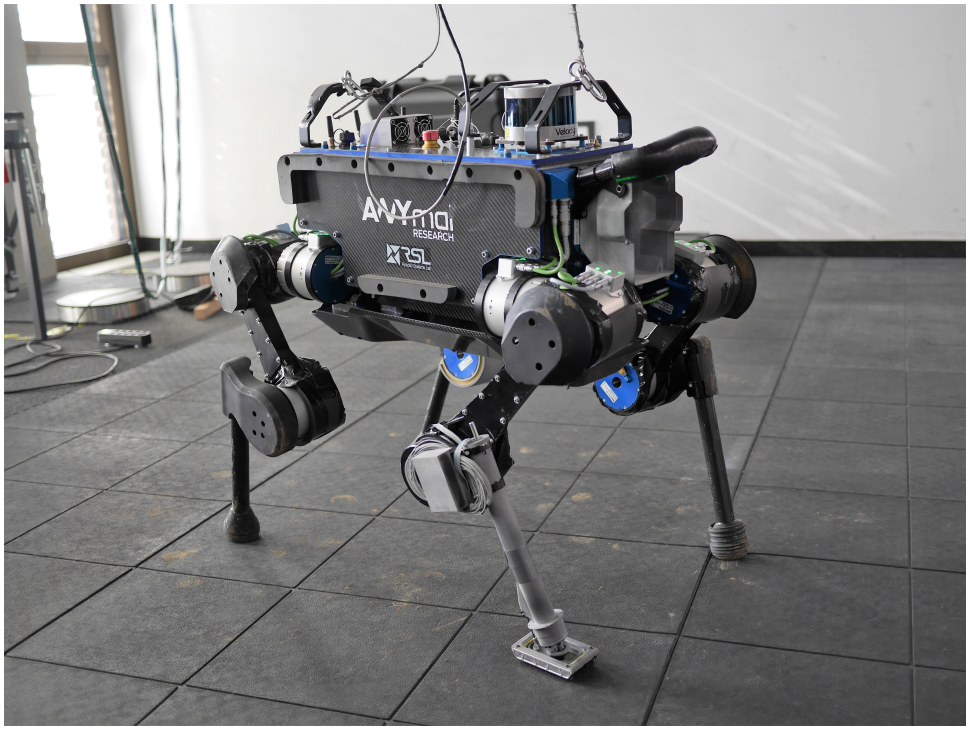

Figure 9.9: Bowden ankle on ANYmal

Chapter 10

Results and Discussion

The test results are summarized in Figure 10.1, where they can be compared with the requirements defined at the start.

Demand Requirements	Minimum Metric	Linear Ankle	Bowden Ankle
Positioning Speed	0.3s	0.1s	0.09s
Positioning Accuracy	~ ±2°	Sufficient	
Pitch ROM	±40°	±50°	±45°
Roll ROM	±30°	±30°	
Impact Robustness	Test on fall machine	TBD	
Lifetime	1 million cycles	TBD, motor OK	
Operating Temperature	0 - 30°C	Motor -30 to +125°C	
Waterproofing	IP67	TBD, should be sufficient	
Low Inertia	0.02 $kg\ m^2$	TBD	Low
Low mass	400g	~375g	~400g
Wish Requirements			
Repairability + Modularity	As high as possible	High	High
Compactness	As high as possible	OK	High
Simplicity	As high as possible	High (+ 17 parts)	Very High (+11 parts)

Figure 10.1: Results for key requirements. Cells shaded in light green exceeded the demanded specifications.

The positioning speed of both ankles substantially exceeded the minimum specification, with safety factors of roughly 3 in both cases.
Their positioning accuracy is not yet final, since later they will additionally be controlled with help of the IMU embedded in the foot. However from manual testing the accuracy is easily sufficient for stepping. Small offsets are automatically eliminated once ANYmal puts its weight on the foot. The pitch ranges are also higher than demanded for both ankles, with the linear ankle gaining an extra 20° over the full range and the bowden ankle an additional 10°. Simultaneously, the roll range of motion is still satisfied.
The durability requirements could not be properly tested yet, because the final metal parts were not available. However the motor is rated at multiple million cycles, so it should last long enough. It also has a very large operating temperature range, so

it will fulfill the temperature requirement. Waterproofing is yet to be tested as well, but should be sufficient, because the ankles use the same waterproofing system as the passive ankle.
Similarly, the inertia is still undetermined, but for the bowden ankle the inertia can not get much lower, because the heaviest component, the motor, is almost as close to the knee joint as possible. The linear ankle's inertia is also lower compared to that of on ankle were the actuator would be inside the joint itself. The ankle masses were estimated in the last chapter and in both cases are within the allowable limit.
Considering the wish requirements, both ankles are very repairable and modular. They are mostly assembled with screws and can thus easily have parts replaced. In both, the motors are also easily accessible for repairs. The linear ankle is inherently modular with the possibility of switching to a larger motor. Whereas the bowden ankle also has distinct subassemblies that can modularly be replaced, such as the tubular motor mount, the cable guide on the shank adapter and the cable anker on the foot.
Furthermore, the linear ankle is sufficiently compact so that it does not get in the way of any of ANYmal's movements. At the same time, the bowden ankle is particularly compact, with only the lower section of the shank and cable protruding outward.
Lastly, both ankles are also very high in simplicity, by using simple actuation and transmission methods. They also have low part counts, with the linear ankle only adding 17 parts, excluding screws, over the passive ankle and the bowden ankle just adding 11.

Chapter 11

Conclusion and Future Work

11.1 Conclusion

In conclusion, both ankles perform very well and fulfill all requirements. They even exceed some requirements, such as the positioning speed and pitch range of motion. Furthermore they also perform well on the wish requirements, providing simple and compact solutions. Thereby they also supply one of the deliverables for the THING project.
Though it does have slightly lower pitching range and is a bit heavier, the bowden ankle has much lower inertia and is significantly more compact compared to the linear ankle. Its bellow is also a lot smaller, so it is less at risk from tearing on some pointy rocks. The motor itself is also more protected directly inside the shank, while only a part of the bowden cable is exposed. And even the cable is quite resilient, being flexible and made from tough metal. If something were to strike the cable, it has some extra compliance when it pulls on and backdrives the motor. Also visually, the bowden ankle has a more sleek and elegant appearance.

11.2 Future Work

For the aforementioned reasons, it is recommended that future work continue on the bowden ankle. Work on the bowden ankle had only begun once the linear ankle was completed, so it is still in prototype form and still has the potential for small improvements.
Firstly, the bellow could be improved by replacing it with one that bends more easily in pitch direction. At the moment, the bellow causes the bowden ankle to heat more quickly at the range limits. A square bellow with folds should remedy this, since the current bellow has to be forced to buckle. Additionally, a small bellow to cover the bowden cable is required. One might use a short one, as found in bicycle brakes, to just cover the bowden cable opening. Or one could use a longer one to cover the entire exposed section. Lastly, a cover for the top of the shank is needed, along with other minor changes.
Next, a more compact controller could be searched for or designed to potentially fit inside the shank. Then the ankle could be integrated with the rest of ANYmal's software, so that it could access the foot and shank IMU data to estimate the ankle joint angle. Additionally it could use the information about whether the foot is in contact when controlling its movement.
Once the ankle is able to move in unison with the legs, ANYmal would be ready for deployment and testing in sewers or mines in the THING project.

Afterwards adding active roll movement could be investigated, by adding a second linear motor to the shank. For this the shank might have to be enlarged.
Lastly, a robotic hand or gripper could be mounted on the end of the ankle, so that the robot could operate handles of machinery or manipulate other objects. It could also grab onto rocks or ledges on steeper terrain and come closer to being able to climb and scale more challenging terrain.

Bibliography

[1] D. Kühn, "Design and development of a hominid robot with local control in its adaptable feet to enhance locomotion capabilities," Tech. Rep., 2016.

[2] C. Piazza, C. Della Santina, G. M. Gasparri, M. G. Catalano, G. Grioli, M. Garabini, and A. Bicchi, "Toward an adaptive foot for natural walking," in *IEEE-RAS International Conference on Humanoid Robots*, 2016.

[3] D. Spenneberg, A. Strack, J. Hilljegerdes, H. Zschenker, M. Albrecht, and F. Kirchner, "ARAMIES: A FOUR-LEGGED CLIMBING AND WALKING ROBOT," 2005.

[4] I. W. Park, J. Y. Kim, J. Lee, and J. H. Oh, "Mechanical design of humanoid robot platform KHR-3 (KAIST humanoid robot - 3: HUBO)," in *Proceedings of 2005 5th IEEE-RAS International Conference on Humanoid Robots*, 2005.

[5] K. Berns, W. Ilg, M. Deck, J. Albiez, and R. Dillmann, "Mechanical construction and computer architecture of the four-legged walking machine BISAM," *IEEE/ASME Transactions on Mechatronics*, vol. 4, no. 1, pp. 32–38, 1999.

[6] E. Garcia, J. C. Arevalo, F. Sanchez, J. F. Sarria, and P. Gonzalez-de Santos, "Design and development of a biomimetic leg using hybrid actuators," in *IEEE International Conference on Intelligent Robots and Systems*, 2011.

[7] N. G. Tsagarakis, Z. Li, J. Saglia, and D. G. Caldwell, "The design of the lower body of the compliant humanoid robot "cCub"," in *Proceedings - IEEE International Conference on Robotics and Automation*, 2011.

[8] R. C. Limón, J. M. I. Zannatha, and M. Á. A. Rodríguez, "Inverse kinematics of a humanoid robot with non-spherical hip: A hybrid algorithm approach: Regular paper," *International Journal of Advanced Robotic Systems*, vol. 10, no. September, 2013.

[9] D. J. Braun, J. E. Mitchell, and M. Goldfarb, "Actuated dynamic walking in a seven-link biped robot," *IEEE/ASME Transactions on Mechatronics*, vol. 17, no. 1, pp. 147–156, 2012.

[10] S. H. Collins and A. Ruina, "A bipedal walking robot with efficient and human-like gait," *Proceedings - IEEE International Conference on Robotics and Automation*, vol. 2005, no. April, pp. 1983–1988, 2005.

[11] S. K. Au, J. Weber, and H. M. Herr, "Biomechanical Design of Powered Ankle-Foot Prosthesis," *Proceedings of the 2007 IEEE 10th International Conference of Rehabilitation Robotics*, vol. 00, no. c, pp. 10–15, 2007.

[12] A. B. Zoss, H. Kazerooni, and A. Chu, "Biomechanical Design of the Berkeley Lower Extremity Exoskeleton (BLEEX)," *TRANSACTIONS ON MECHATRONICS*, vol. 11, no. 2, 2006.

[13] M. Fujino, "Design and Development of the Biped Prototype Robian," 2002.

[14] R. D. Bellman, M. A. Holgate, and T. G. Sugar, *SPARKy 3: Design of an Active Robotic Ankle Prosthesis with Two Actuated Degrees of Freedom Using Regenerative Kinetics*, 2008.

[15] J. Wheeler, H. Krebs, and N. Hogan, "An ankle robot for a modular gait rehabilitation system," *2004 IEEE/RSJ International Conference on Intelligent Robots and Systems (IROS) (IEEE Cat. No.04CH37566)*, vol. 2, pp. 1680–1684, 2004.

[16] C. Lovchik and M. Diftler, "The Robonaut hand: a dexterous robot hand for space," *Proceedings 1999 IEEE International Conference on Robotics and Automation (Cat. No.99CH36288C)*, vol. 2, no. May, pp. 907–912, 1999.

[17] Y. Fan and Y. Yin, "Mechanism design and motion control of a parallel ankle joint for rehabilitation robotic exoskeleton," in *2009 IEEE International Conference on Robotics and Biomimetics, ROBIO 2009*, 2009.

[18] C. Lataniotis, "Optimizing dynamic motions of two-link pendulum," p. 42, 2011.

[19] J. Wüthrich, "Dimensionieren I, Zusammenfassung," [Online]. Available: https://legacy.amiv.ethz.ch/studium/unterlagen, 16.4.2019.

Appendix A

Connection Diagram

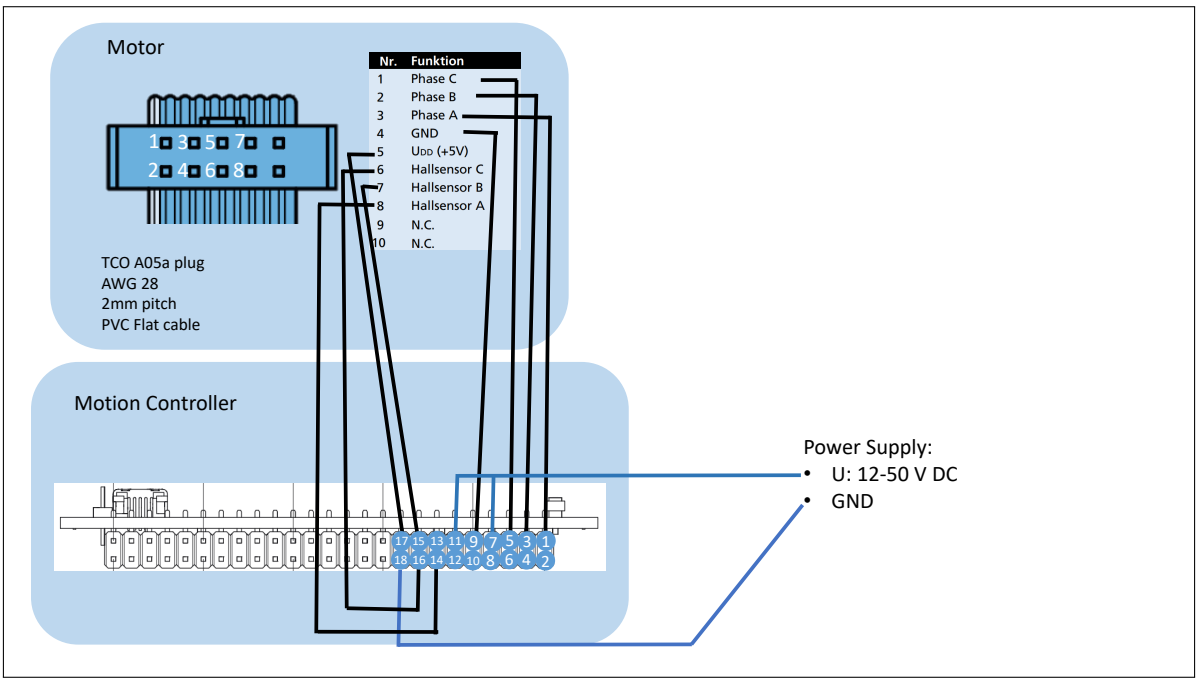
Motor
Nr. Funktion
1 Phase C
2 Phase B
3 Phase A
4 GND
5 UDD (+5V)
6 Hallsensor C
7 Hallsensor B
8 Hallsensor A
9 N.C.
10 N.C.
1 3 5 7
2 4 6 8
TCO A05a plug
AWG 28
2mm pitch
PVC Flat cable
Motion Controller
17 15 13 11 9 7 5 3 1
18 16 14 12 10 8 6 4 2
Power Supply:
• U: 12-50 V DC
• GND

Appendix B

Datasheets

EC 13 ∅13 mm, brushless, 12 Watt

A with Hall sensors

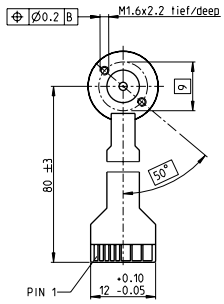

B sensorless

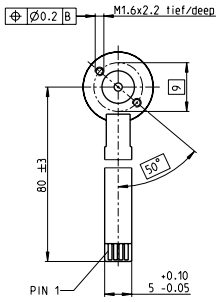

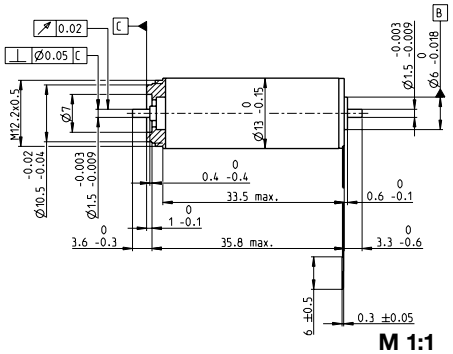

M 1:1

Stock program
Standard program
Special program (on request)

	Part Numbers					
A with Hall sensors	426397	430160	430161	430162	430163	430164
B sensorless	426576	430166	430167	430168	430169	430170

Motor Data								
Values at nominal voltage								
1 Nominal voltage	V	6	9	12	18	24	36	
2 No load speed	rpm	24100	24200	24100	24900	24100	26600	
3 No load current	mA	198	132	98.9	68.9	49.5	38.2	
4 Nominal speed	rpm	18200	19100	18800	20000	19000	21700	
5 Nominal torque (max. continuous torque)	mNm	5.15	5.64	5.13	5.53	5.18	5.38	
6 Nominal current (max. continuous current)	A	2.37	1.72	1.18	0.871	0.598	0.456	
7 Stall torque	mNm	21.7	27.4	23.8	28.8	24.8	30.3	
8 Stall current	A	9.31	7.85	5.1	4.24	2.67	2.38	
9 Max. efficiency	%	74	76	75	77	75	77	
Characteristics								
10 Terminal resistance phase to phase	Ω	0.644	1.15	2.35	4.24	9	15.1	
11 Terminal inductance phase to phase	mH	0.0103	0.0233	0.0413	0.0879	0.165	0.308	
12 Torque constant	mNm/A	2.33	3.49	4.66	6.8	9.32	12.7	
13 Speed constant	rpm/V	4100	2730	2050	1410	1020	751	
14 Speed/torque gradient	rpm/mNm	1130	896	1030	877	990	893	
15 Mechanical time constant	ms	3.86	3.05	3.52	2.99	3.37	3.04	
16 Rotor inertia	gcm²	0.325	0.325	0.325	0.325	0.325	0.325	

Specifications

Thermal data

17	Thermal resistance housing-ambient	23.9 K/W
18	Thermal resistance winding-housing	1.26 K/W
19	Thermal time constant winding	0.603 s
20	Thermal time constant motor	263 s
21	Ambient temperature	-40…+100°C
22	Max. winding temperature	+155°C

Mechanical data (preloaded ball bearings)

23	Max. speed		50000 rpm
24	Axial play at axial load	< 1.8 N	0 mm
		> 1.8 N	max. 0.05 mm
25	Radial play		preloaded
26	Max. axial load (dynamic)		1.5 N
27	Max. force for press fits (static)		18 N
	(static, shaft supported)		250 N
28	Max. radial load, 5 mm from flange		4 N

Other specifications

29	Number of pole pairs	1
30	Number of phases	3
31	Weight of motor	29 g

Connection	with Hall sensors	sensorless
Pin 1	V_{Hall} 4.5…24 VDC	Motor winding 1
Pin 2	Hall sensor 3	Motor winding 2
Pin 3	Hall sensor 1	Motor winding 3
Pin 4	Hall sensor 2	N.C.
Pin 5	GND	
Pin 6	Motor winding 3	
Pin 7	Motor winding 2	
Pin 8	Motor winding 1	

Adapter	Part number	Part number
see p. 471	220300	220310
Connector	**Part number**	**Part number**
Tyco	1-84953-1	84953-4
Molex	52207-1133	52207-0433
Molex	52089-1119	52089-0419

Pin for design with Hall sensors:
FPC, 11-pol, Pitch 1.0 mm, top contact style
Wiring diagram for Hall sensors see page 41

Operating Range

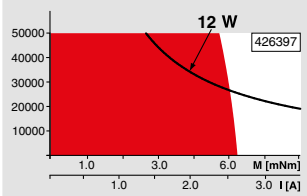

Comments

Continuous operation
In observation of above listed thermal resistance (lines 17 and 18) the maximum permissible winding temperature will be reached during continuous operation at 25°C ambient.
= Thermal limit.

Short term operation
The motor may be briefly overloaded (recurring).

Assigned power rating

maxon Modular System

Overview on page 28–36

Planetary Gearhead
∅13 mm
0.2 - 0.35 Nm
Page 323

Recommended Electronics:

Notes	Page **32**
ESCON Module 24/2	444
ESCON 36/3 EC	445
ESCON Mod. 50/4 EC-S	445
ESCON Module 50/5	445
ESCON 50/5	447
DEC Module 24/2	449
DEC Module 50/5	449

Planetary Gearhead GP 13 A ∅13 mm, 0.2–0.35 Nm

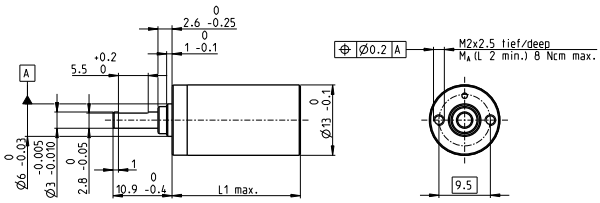

M 1:1

Technical Data

Planetary Gearhead	straight teeth
Output shaft	stainless steel, hardened
Bearing at output	sleeve bearing
Radial play, 6 mm from flange	max. 0.055 mm
Axial play	0.02–0.10 mm
Max. axial load (dynamic)	8 N
Max. force for press fits	100 N
Direction of rotation, drive to output	=
Max. continuous input speed	8000 rpm
Recommended temperature range	-40…+100°C
Number of stages	1 2 3 4 5
Max. radial load, 6 mm from flange	8 N 12 N 16 N 20 N 20 N

Stock program
Standard program
Special program (on request)

			Part Numbers				
			110313	110314	110315	110316	110317
Gearhead Data							
1	Reduction		4.1:1	17:1	67:1	275:1	1119:1
2	Absolute reduction		57/14	3249/196	185193/2744	10556001/38416	601692057/537824
3	Max. motor shaft diameter	mm	1.5	1.5	1.5	1.5	1.5
	Part Numbers		352365	352366	352367	352368	352369
1	Reduction		5.1:1	26:1	131:1	664:1	3373:1
2	Absolute reduction		66/13	4356/169	287496/2197	18974736/28561	1252332576/371293
3	Max. motor shaft diameter	mm	1.5	1.5	1.5	1.5	1.5
4	Number of stages		1	2	3	4	5
5	Max. continuous torque	Nm	0.20	0.20	0.30	0.30	0.35
6	Max. intermittent torque at gear output	Nm	0.30	0.30	0.45	0.45	0.53
7	Max. efficiency	%	91	83	75	69	62
8	Weight	g	11	14	17	20	23
9	Average backlash no load	°	1.0	1.2	1.5	1.8	2.0
10	Mass inertia	gcm²	0.025	0.015	0.015	0.015	0.015
11	Gearhead length L1*	mm	16.0	19.9	23.7	27.6	31.4

* for A-max 12 is L1 + 0.3 mm

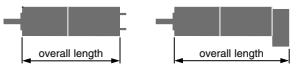

maxon Modular System

+ Motor	Page	+ Sensor/Brake	Page	Overall length [mm] = Motor length + gearhead length + (sensor/brake) + assembly parts				
RE 13	105/107			35.4	39.3	43.1	47.0	50.8
RE 13, 0.75 W	107	MR	413-415	42.5	46.4	50.2	54.1	57.9
RE 13, 0.75 W	107	MEnc 13	407	43.2	47.1	50.9	54.8	58.6
RE 13	109/111			47.6	51.5	55.3	59.2	63.0
RE 13, 2 W	111	MR	413-415	54.7	58.6	62.4	66.3	70.1
RE 13, 2 W	111	MEnc 13	407	55.4	59.3	63.1	67.0	70.8
RE 13, 1.5 W	113/115			38.5	42.4	46.2	50.1	53.9
RE 13, 1.5 W	115	MR	413-415	44.6	48.5	52.3	56.2	60.0
RE 13, 1.5 W	115	MEnc 13	407	46.5	50.4	54.2	58.1	61.9
RE 13, 3 W	117/119			50.7	54.6	58.4	62.3	66.1
RE 13, 3 W	119	MR	413-415	56.8	60.7	64.5	68.4	72.2
RE 13, 3 W	119	MEnc 13	407	58.7	62.6	66.4	70.3	74.1
A-max 12	137/138			37.6	41.5	45.3	49.2	53.0
A-max 12, 0.5 W	138	MR	413-415	41.7	45.6	49.4	53.3	57.1
EC 13, 6 W	208			37.4	41.3	45.1	49.0	52.8
EC 13, 12 W	209			49.6	53.5	57.3	61.2	65.0

Option Ball Bearing

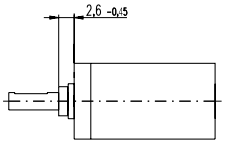

Gearhead length: L1 + 0.2 mm

Part Numbers

4.1 : 1	144300	131 : 1	352393
5.1 : 1	352391	275 : 1	144303
17 : 1	144301	664 : 1	352394
26 : 1	352392	1119 : 1	144304
67 : 1	144302	3373 : 1	352395

Technical Data

Planetary Gearhead	straight teeth
Output shaft	stainless steel, hardened
Bearing at output	preloaded ball bearings
Radial play, 6 mm from flange	max. 0.04 mm
Axial play at axial load	< 5 N 0 mm
	> 5 N max. 0.04 mm
Max. axial load (dynamic)	8 N
Max. force for press fits	25 N
Direction of rotation, drive to output	=
Max. continuous input speed	8000 rpm
Recommended temperature range	-40…+100°C
Number of stages	1 2 3 4 5
Max. radial load, 6 mm from flange	10 N 15 N 20 N 25 N 25 N

Gearhead values according to sleeve bearing version

EC 45 flat ∅42.9 mm, brushless, 30 Watt

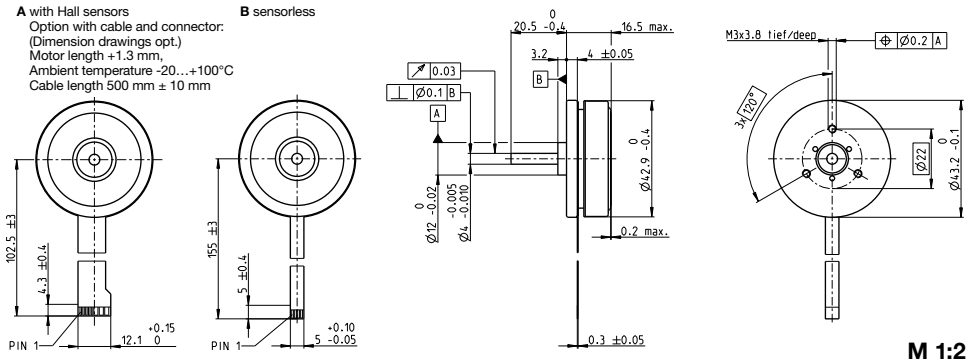

M 1:2

Stock program
Standard program
Special program (on request)

	Part Numbers					
A with Hall sensors	200142		339281		339282	
Option with Cable and Connector	387266		400527		400580	
B sensorless		200189		339283		339284
Motor Data						
Values at nominal voltage						
1 Nominal voltage V	12	12	24	24	36	36
2 No load speed rpm	4370	4350	4360	4380	4750	4760
3 No load current mA	163	163	81.4	73	61.6	55.3
4 Nominal speed rpm	2940	2800	2940	2900	3290	3270
5 Nominal torque (max. continuous torque) mNm	55	54.7	54.8	55.2	66	66.6
6 Nominal current (max. continuous current) A	2.02	2.02	1.01	1.01	0.847	0.849
7 Stall torque[1] mNm	255	219	253	243	380	369
8 Stall current A	10	8.58	4.97	4.77	5.38	5.22
9 Max. efficiency %	76	75	76	77	80	81
Characteristics						
10 Terminal resistance phase to phase Ω	1.2	1.4	4.83	5.03	6.69	6.89
11 Terminal inductance phase to phase mH	0.56	0.56	2.24	2.24	4.29	4.29
12 Torque constant mNm/A	25.5	25.5	51	51	70.6	70.6
13 Speed constant rpm/V	374	374	187	187	135	135
14 Speed/torque gradient rpm/mNm	17.6	20.5	17.7	18.5	12.8	13.2
15 Mechanical time constant ms	17.1	19.9	17.2	17.9	12.4	12.8
16 Rotor inertia gcm²	92.5	92.5	92.5	92.5	92.5	92.5

Specifications

Thermal data

17	Thermal resistance housing-ambient	6.69 K/W
18	Thermal resistance winding-housing	3.92 K/W
19	Thermal time constant winding	11.4 s
20	Thermal time constant motor	295 s
21	Ambient temperature	-40…+100°C
22	Max. winding temperature	+125°C

Mechanical data (preloaded ball bearings)

23	Max. speed		10000 rpm
24	Axial play at axial load	< 5.0 N	0 mm
		> 5.0 N	typ. 0.14 mm
25	Radial play		preloaded
26	Max. axial load (dynamic)		4.8 N
27	Max. force for press fits (static)		53 N
	(static, shaft supported)		1000 N
28	Max. radial load, 5 mm from flange		18 N

Other specifications

29	Number of pole pairs	8
30	Number of phases	3
31	Weight of motor	75 g

Values listed in the table are nominal.

Connection	with Hall sensors	sensorless
Pin 1	V_{Hall} 4.5…18 VDC	Motor winding 1
Pin 2	Hall sensor 3*	Motor winding 2
Pin 3	Hall sensor 1*	Motor winding 3
Pin 4	Hall sensor 2*	⅄ neutral point
Pin 5	GND	
Pin 6	Motor winding 3	
Pin 7	Motor winding 2	
Pin 8	Motor winding 1	

*Internal pull-up (7…13 kΩ) on V_{Hall}

Wiring diagram for Hall sensors see p. 43

Adapter	Part number	Part number
see p. 471	220300	220310
Connector	**Part number**	**Part number**
Tyco	1-84953-1	84953-4
Molex	52207-1133	52207-0433
Molex	52089-1119	52089-0419

Pin for design with Hall sensors:
FPC, 11-pol, Pitch 1.0 mm, top contact style
[1]Calculation does not include saturation effect (p. 53/164)

Operating Range

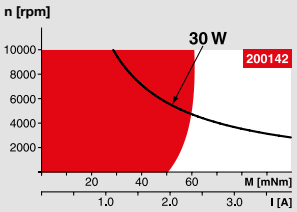

Comments

Continuous operation
In observation of above listed thermal resistance (lines 17 and 18) the maximum permissible winding temperature will be reached during continuous operation at 25°C ambient.
= Thermal limit.

Short term operation
The motor may be briefly overloaded (recurring).

Assigned power rating

maxon Modular System

Overview on page 28–36

Planetary Gearhead
∅42 mm
3 - 15 Nm
Page 356

Spur Gearhead
∅45 mm
0.5 - 2.0 Nm
Page 358

Recommended Electronics:

Notes	Page 32
ESCON Module 24/2	444
ESCON 36/3 EC	445
ESCON Mod. 50/4 EC-S	445
ESCON Module 50/5	445
ESCON 50/5	447
DEC Module 24/2	449
DEC Module 50/5	449
EPOS4 Mod./Comp. 24/1.5	452
EPOS4 50/5	453
EPOS4 Mod./Comp. 50/5	453
EPOS2 P 24/5	464
MAXPOS 50/5	468

for motor type A:
Encoder MILE
256 - 2048 CPT,
2 channels
Page 402

FAULHABER

Linear DC-Servomotors 3,6 N

with Analog Hall Sensors

LM 1247 ... 11

Values at 22°C	LM 1247 ... 11		
Continuous force	$F_{e\,max.}$	3,6	N
Peak force	$F_{p\,max.}$	10,7	N
Continuous current	$I_{e\,max.}$	0,55	A
Peak current	$I_{p\,max.}$	1,66	A
Back-EMF constant	k_E	5,25	V/m/s
Force constant	k_F	6,43	N/A
Terminal resistance, phase-phase	R	13,17	Ω
Terminal inductance, phase-phase	L	820	µH
Thermal resistance	R_{th1} / R_{th2}	3,2 / 20	K/W
Thermal time constant	τ_{w1} / τ_{w2}	11 / 624	s
Operating temperature range		-20 … +125	°C
Magnetic pitch	τ_m	18	mm
Rod bearings		polymer sleeves	
Housing material		metal, non-magnetic	
Direction of movement		electronically reversible	

	LM 1247-	020-11	040-11	060-11	080-11	100-11	120-11	
Stroke length	$S_{max.}$	20	40	60	80	100	120	mm
Repeatability	σ_r	40	40	40	40	40	40	µm
Accuracy	σ_a	120	140	160	180	200	220	µm
Acceleration	$a_{e\,max.}$	198	148,5	127,3	101,8	91,4	82,9	m/s²
Speed	$v_{e\,max.}$	2	2,4	2,8	2,9	3	3,2	m/s
Rod length	$L1$	82	109	127	154	172	190	mm
Rod mass	m_m	18	24	28	35	39	43	g
Total mass	m_t	57	63	67	74	78	82	g

Note: These motors are for operation with DC-voltage < 75 V DC. The given values are for free standing motors.
Other rod lengths available on request.

Motor characteristic curves

Trapezoidal motion profile (t1 = t2 = t3)

Displacement distance:	20 mm
Friction coefficient:	0,2
Slope angle:	0°
Rest time:	0,1 s

Load:
The max. applicable load (incl. rod) at a given speed with an external force of 0 N

External force:
The max. permissible external force at a given speed with a load (incl. rod) of:

- 0,1 kg
- 0,2 kg
- 0,5 kg

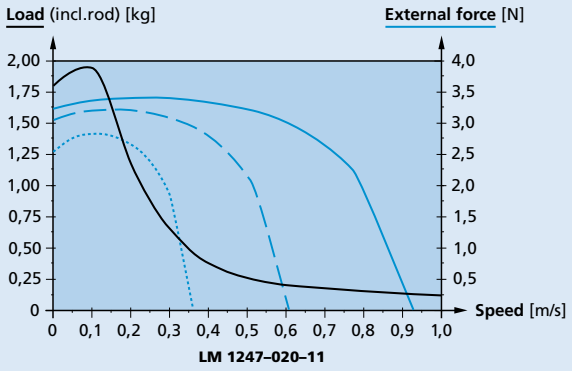

LM 1247–020–11

For notes on technical data and lifetime performance refer to "Technical Information".

Edition 2019

FAULHABER

Dimensional drawing

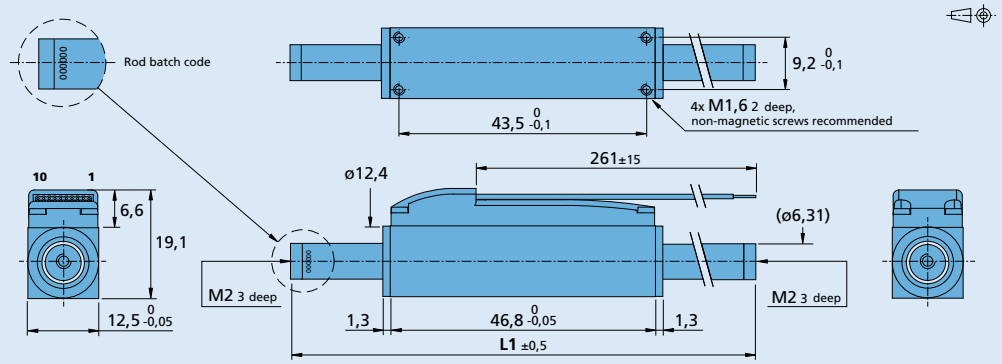

LM 1247 ... 11

Option, cable and connection information

Example product designation: **LM1247-020-11**

Option	Type	Description
-11C	Connector 	Material PVC, 10 conductors, AWG 28 with connector A05a - TCO, pitch 2 mm
-01	Single wires	Material PVC, 10 conductors, AWG 28. Recommended connector: Molex - Nr. 51110-1060

Connection

-11/-11C		-01		
No.	Function	No.	Function	Color
1	Phase C	1	Phase C	yellow
2	Phase B	2	Hall sensor A	green
3	Phase A	3	U_{DD} (+5V)	red
4	GND	4	GND	black
5	U_{DD} (+5V)	5	Hall sensor B	blue
6	Hall sensor C	6	Hall sensor C	grey
7	Hall sensor B	7	Phase B	orange
8	Hall sensor A	8	Phase A	brown
9	N.C.	9	N.C.	white
10	N.C.	10	N.C.	purple

Standard cable

Material PVC,
10 conductors, AWG 28,
grid 1mm, wires tinned.

Product combination

Drive Electronics

MCLM 3002 P
MCLM 3002 S
MCLM 3003 P
MCLM 3006 S
MC 5004 P
MC 5004 P STO
MC 5005 S

Cables / Accessories

To view our large range of accessory parts, please refer to the "Accessories" chapter.

FAULHABER

Linear DC-Servomotors 6,2 N

with Analog Hall Sensors

LM 1483 ... 11

Values at 22°C	LM 1483 ... 11		
Continuous force	$F_{e\,max.}$	6,2	N
Peak force	$F_{p\,max.}$	18,4	N
Continuous current	$I_{e\,max.}$	0,5	A
Peak current	$I_{p\,max.}$	1,48	A
Back-EMF constant	k_E	10,16	V/m/s
Force constant	k_F	12,44	N/A
Terminal resistance, phase-phase	R	26,3	Ω
Terminal inductance, phase-phase	L	1 649	µH
Thermal resistance	R_{th1} / R_{th2}	1,97 / 12,5	K/W
Thermal time constant	τ_{w1} / τ_{w2}	12,2 / 789	s
Operating temperature range		-20 … +125	°C
Magnetic pitch	τ_m	18	mm
Rod bearings		polymer sleeves	
Housing material		metal, non-magnetic	
Direction of movement		electronically reversible	

	LM 1483-	020-11	040-11	060-11	080-11	
Stroke length	$S_{max.}$	20	40	60	80	mm
Repeatability	σ_r	40	40	40	40	µm
Accuracy	σ_a	120	140	160	180	µm
Acceleration	$a_{e\,max.}$	220,7	176,6	158,5	143,7	m/s²
Speed	$v_{e\,max.}$	2,1	2,7	3,1	3,4	m/s
Rod length	$L1$	127	154	172	190	mm
Rod mass	m_m	28	35	39	43	g
Total mass	m_t	117	124	128	132	g

Note: These motors are for operation with DC-voltage < 75 V DC. The given values are for free standing motors.
Other rod lengths available on request.

Motor characteristic curves

Trapezoidal motion profile (t1 = t2 = t3)

Displacement distance:	20 mm
Friction coefficient:	0,2
Slope angle:	0°
Rest time:	0,1 s

Load:
The max. applicable load (incl. rod) at a given speed with an external force of 0 N

External force:
The max. permissible external force at a given speed with a load (incl. rod) of:

- 0,15 kg
- 0,3 kg
- 0,6 kg

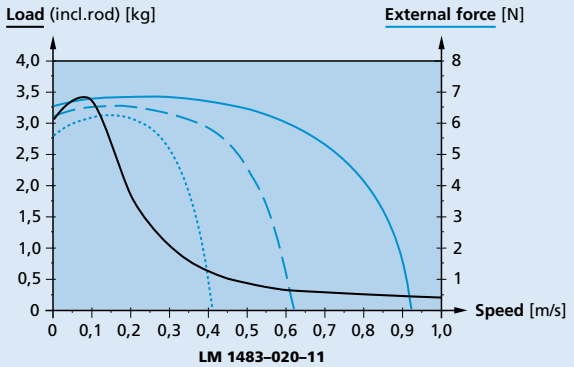

LM 1483–020–11

For notes on technical data and lifetime performance refer to "Technical Information".

Edition 2019 Feb. 13

FAULHABER

Dimensional drawing

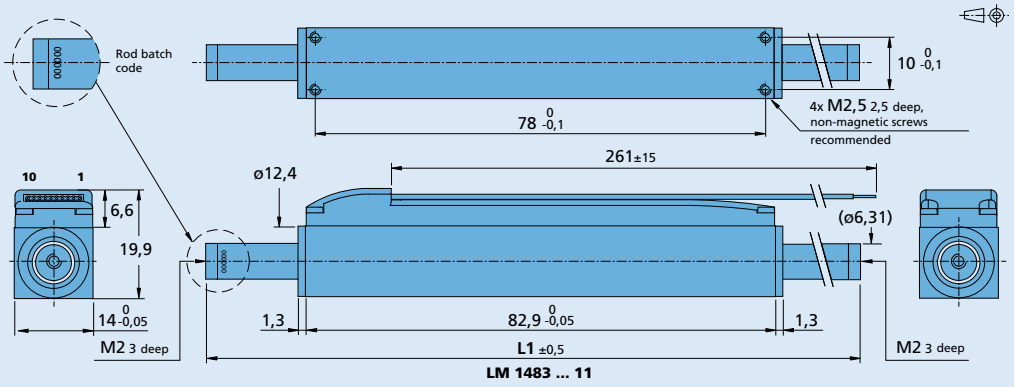

LM 1483 ... 11

Option, cable and connection information

Example product designation: **LM1483-020-11**

Option	Type	Description
-11C	Connector 	Material PVC, 10 conductors, AWG 28 with connector A05a - TCO, pitch 2 mm

Connection -11/-11C

No.	Function
1	Phase C
2	Phase B
3	Phase A
4	GND
5	U_{DD} (+5V)
6	Hall sensor C
7	Hall sensor B
8	Hall sensor A
9	N.C.
10	N.C.

Standard cable

Material PVC,
10 conductors, AWG 28,
grid 1mm, wires tinned.

Product combination

Drive Electronics

MCLM 3002 P
MCLM 3002 S
MCLM 3003 P
MCLM 3006 S
MC 5004 P
MC 5004 P STO
MC 5005 S

Cables / Accessories

To view our large range of accessory parts, please refer to the "Accessories" chapter.

For notes on technical data and lifetime performance refer to "Technical Information".

Edition 2019 Feb. 13

FAULHABER

Motion Controllers

V3.0, 4-Quadrant PWM
with RS232, CANopen or EtherCAT interface

MC 5004 P

Values at 22°C		MC 5004 P	
Power supply electronic	U_P	12 ... 50	V DC
Power supply motor	U_{mot}	0 ... 50	V DC
PWM switching frequency	f_{PWM}	100	kHz
Efficiency electronic	η	95	%
Max. continuous output current	I_{cont}	4	A
Max. peak output current [1]	I_{max}	12	A
Standby current for electronic (at U_P=24V)	I_{el}	RS / CO: 0,06 ET: 0,07	A
Operating temperature range		-40 ... +85	°C
Mass		RS / CO: 22 ET: 47	g

[1] S2 mode for max. 1s

Interfaces	MC 5004 P RS/CO	MC 5004 P ET
Configuration from Motion Manager 6.0	RS232 / USB	RS232 / USB
Fieldbus	RS232 / CANopen	EtherCAT

Basic features

- Control of brushless, DC- and linear motors
- Supported sensor systems: absolute encoders (AES or SSI), incremental encoders (optical or magnetic), Hall sensors (digital or analog), tachometers
- Positioning resolution when using analog Hall sensors as position encoder: 4096 increments per revolution
- 8 digital inputs, 3 digital outputs, 2 analog inputs, flexible configuration
- Setpoint specification via fieldbus, quadrature signal, pulse and direction or analog inputs
- Optional stand-alone operation via application programs in all interface versions

Range of functions

Operating modes	PP, PV, PT, CSP, CSV, CST and homing acc. to IEC 61800-7-201 or IEC 61800-7-301 as well as position-, speed- and torque control via analog setpoint or voltage controller
Speed range for brushless motors with number of pole pairs 1	0 min^{-1} ... 30 000 min^{-1} with sinusoidal commutation (optionally to 60 000 min^{-1} with block commutation)
Application programs	Max. 8 application programs (BASIC), one of which is an autostart function
Additional functions	Touch-probe input, connection of a second incremental encoder, control of a holding brake
Indicator	LEDs for displaying the operating state Trace as recorder (scope function) or logger
Motor types	DC, BL- and linear motors

For notes on technical data and lifetime performance refer to "Technical Information".

Edition 2019 Mar. 08

FAULHABER

Dimensional drawing

Scale reduced

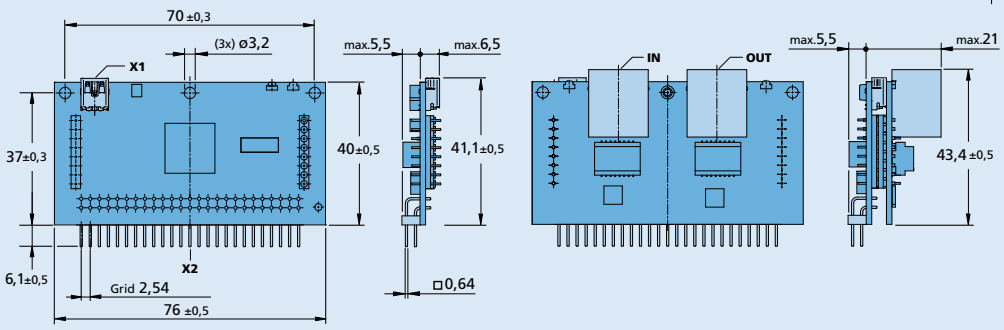

MC 5004 P RS/CO **MC 5004 P ET**

Options and connection information

Example product designation: **MC 5004 P ET FC**

Option	Type	Description
FC	EtherCAT IN/OUT 	Interface connector DIN, for use in combination with flat cables (see chapter "accessories")
5621	Multi-pin connector	Horizontal PCB assembly

Connection

Name	Function	Description
X1	USB configuration interface	USB
X2	Pin Header	Analog and digital input/output, motor and eletronic, power supply, fieldbus, motor phases, sensors
IN	Fieldbus	EtherCAT IN
OUT	Fieldbus	EtherCAT OUT

Note: For details on the connection assignment, see device manual for the MC 5004.

Product combination

DC-Motors	Brushless DC-Motors	Linear DC-Servomotors	Cables / Accessories
1319 ... SR 1331 ... SR 1336 ... CXR 1516 ... SR 1524 ... SR 1717 ... SR 1724 ... SR 1727 ... CXR 1741 ... CXR 2224 ... SR 2232 ... SR 2237 ... CXR 2342 ... CR 2642 ... CR 2642 ... CXR 2657 ... CR 2657 ... CXR 2668 ... CR	1218 ... B 1226 ... B 1628 ... B 1645 ... BHS 1660 ... BHT 2036 ... B 2057 ... B 2214 ... BXT H 2232 ... BX4 2250 ... BX4 2250 ... BX4 S 2444 ... B 3056 ... B 3216 ... BXT H 3242 ... BX4 3268 ... BX4 4221 ... BXT H	LM 0830 ... 01 LM 1247 ... 11 LM 1483 ... 11 LM 2070 ... 11	An extensive range of accessories is available for the products of the MC 5004 controller series. A motherboard is available that can be used to operate up to four controllers in multi-axis operation (slave). Furthermore, connection cables are available for controller and motor supply, sensors and interfaces as well as connector sets for the motor and supply side. To view our large range of accessory parts, please refer to the „Accessories" chapter.

For notes on technical data and lifetime performance refer to "Technical Information".

Edition 2019 Mar. 08